Stock assessment

1st season 2018

Doryteuthis gahi

Andreas Winter

Natural Resources

Fisheries

June 2018

Index

Summary

1) The 2018 first season *Doryteuthis gahi* fishery (C license) was open from February 27th, and closed by directed order on May 1st. Compensatory days for mechanical problems and bad weather resulted in 38 vessel-days taken after May 1st, with one vessel fishing as late as May 6th.
2) Four fishing mortalities of Southern sea lions and two fishing mortalities of South American fur seals were recorded throughout the course of the season, resulting in mandatory use of Seal Exclusion Devices north of 52° S starting on April 26th, and south of 52° S starting on May 3rd.
3) 43,085 tonnes of *D. gahi* catch were reported in the C-license fishery; the highest 1st season catch since 1995 and giving an average CPUE of 44.2 t vessel-day^{-1}. During the season 75.1%% of *D. gahi* catch and 69.2% of fishing effort were taken north of 52º S; 24.9% of *D. gahi* catch and 30.8% of fishing effort were taken south of 52º S. The bias to the north was partially dictated by temporary closures in the south, to allow the squid more growth.
4) In the north sub-area, four depletion periods / immigrations were inferred to have started on February 27th (start of the season), March 5th, March 16th, and March 28th. In the south sub-area, five depletion periods / immigrations were inferred to have started on February 27th, March 1st, March 14th, April 8th, and April 30th.
5) Approximately 74,043 tonnes of *D. gahi* (95% confidence interval: 58,689 to 124,487 t) were estimated to have immigrated into the Loligo Box during first season 2018, of which 59,278 t north of 52º S and 14,765 t south of 52º S.
6) The escapement biomass estimate for *D. gahi* remaining in the Loligo Box at the end of first season 2018 was:

   Maximum likelihood of 31,356 tonnes, with a 95% confidence interval of 24,140 to 65,208 tonnes.

   The risk of *D. gahi* escapement biomass at the end of the season being less than 10,000 tonnes was estimated at effectively zero.

Introduction

Start of the first season of the 2018 *Doryteuthis gahi* fishery (Patagonian longfin squid – colloquially *Loligo*) was postponed from February 24th to February 26th, to allow for contract observers to arrive on the February 24th (Saturday) LATAM flight. This flight was then weather-delayed for a day and the start of the season postponed again to February 27th. Thus, for a combination of different reasons, the 1st season schedule became identical to the year before (Winter 2017a). Fourteen C-licensed trawlers started the season on February 27th. One trawler delayed entry by one day for mechanical repairs, and one trawler delayed entry as it was replacing a damaged vessel. In total during the season, 4 flex days were taken for mechanical repairs by various vessels. Every vessel took at least 1 bad-weather day for a fleet total of 38 bad-weather days, including 2 days on which no vessels fished (Figure 1). The season ended by directed closure on May 1st. The various schedule adjustments amounted to 38 vessel-days being taken after May 1st[a], with the last vessels finishing on May 6th.

Total reported *D. gahi* catch under first season C license was 43,085 tonnes (Table 1), the highest since 1995, and corresponding to an average CPUE of 43085 / 975 = 44.2 tonnes vessel-day^{-1}. Average CPUE was the highest in a first season since 2012.

[a] One vessel with a partial season allocation expended its flex days earlier than May 1st.

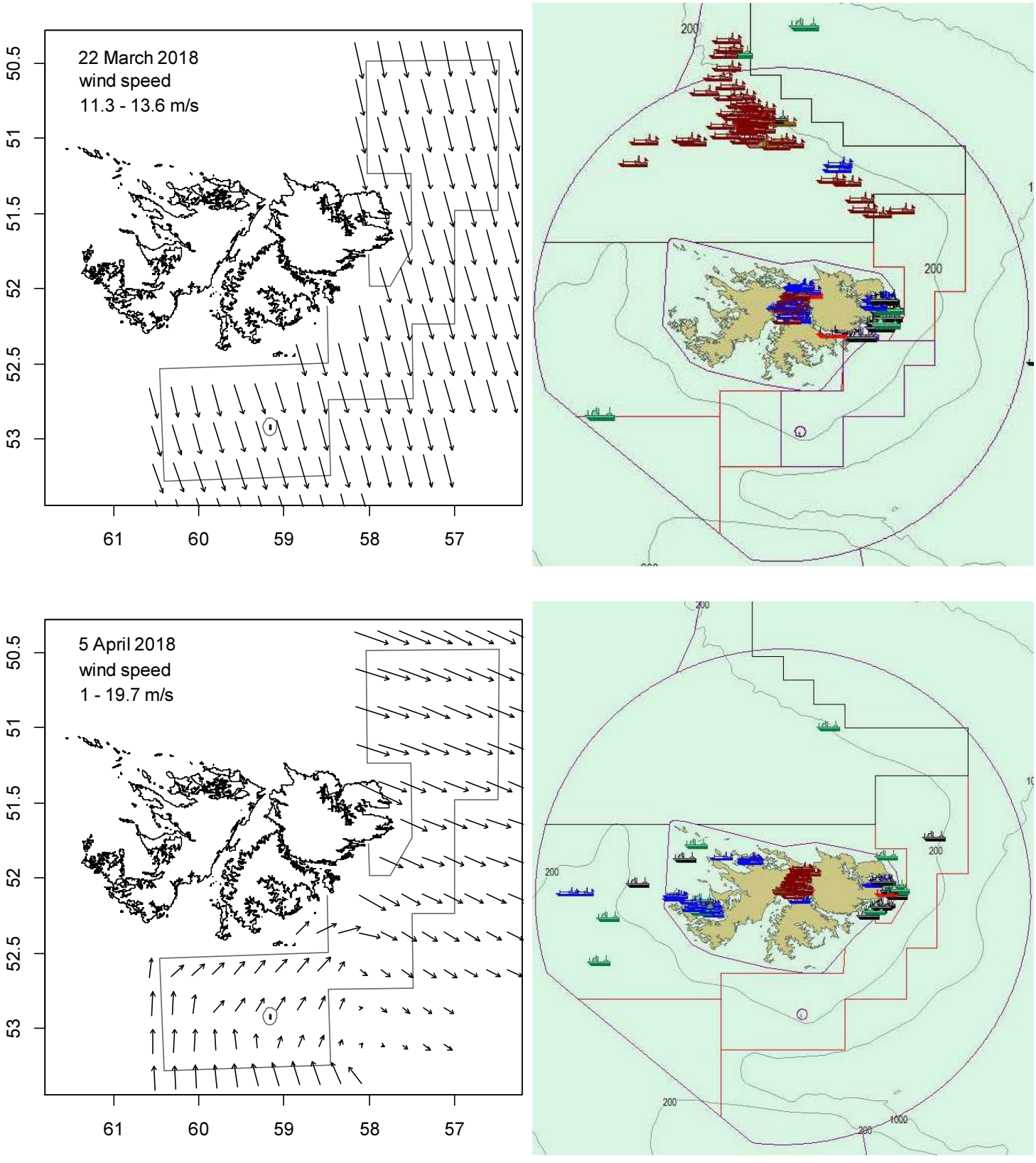

Figure 1. Left: wind speed vector plot at 0.25° resolution, from blended satellite observations (Zhang et al., 2006). Right: Fish Ops chart display. Top: March 22nd, when no C-licensed vessels fished, bottom: April 5th, when no C-licensed vessels fished.

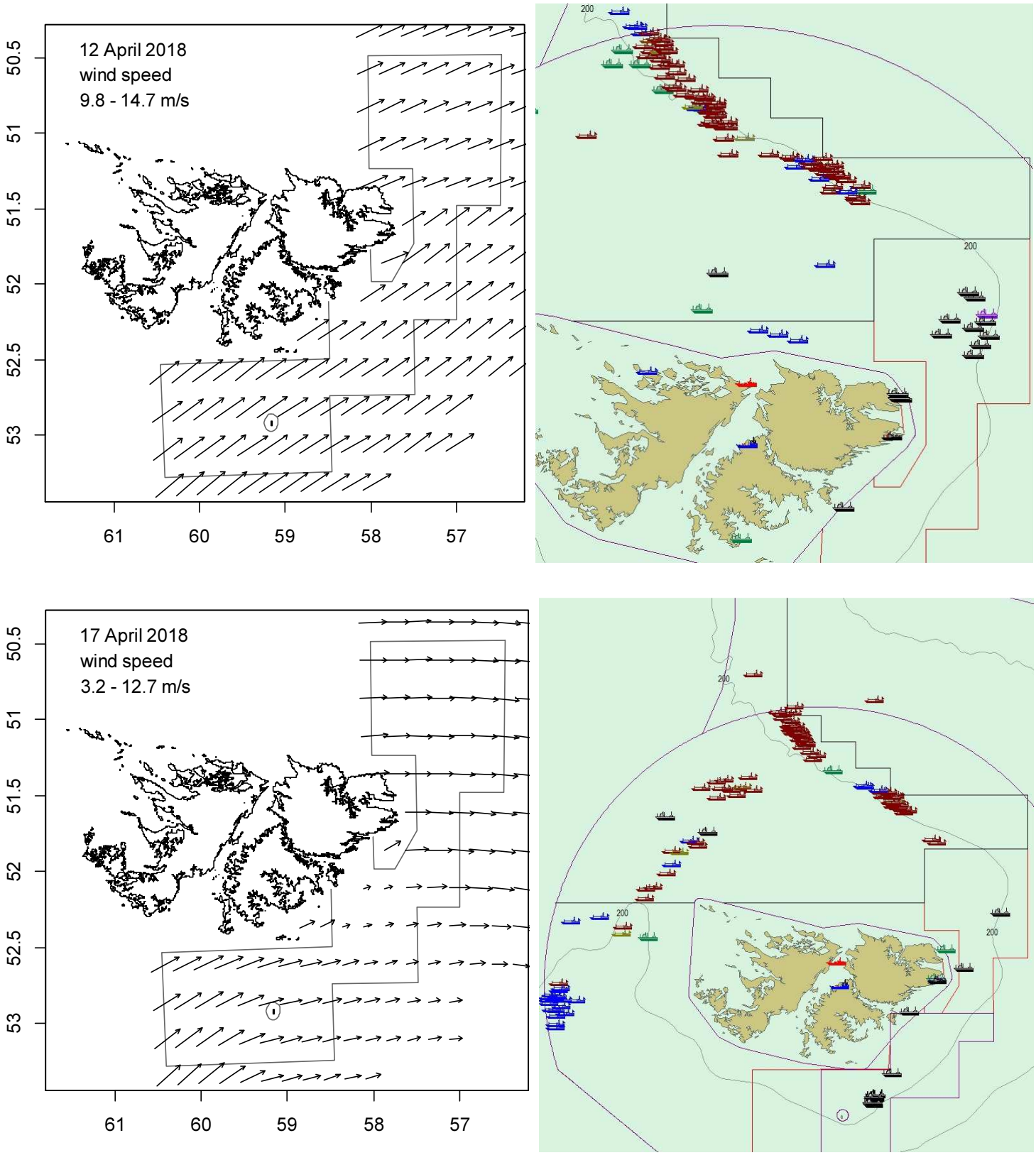

Figure 1 (continued). Top: April 12th, when 6 vessels declared bad-weather days, bottom: April 17th, when 3 vessels declared a bad-weather day.

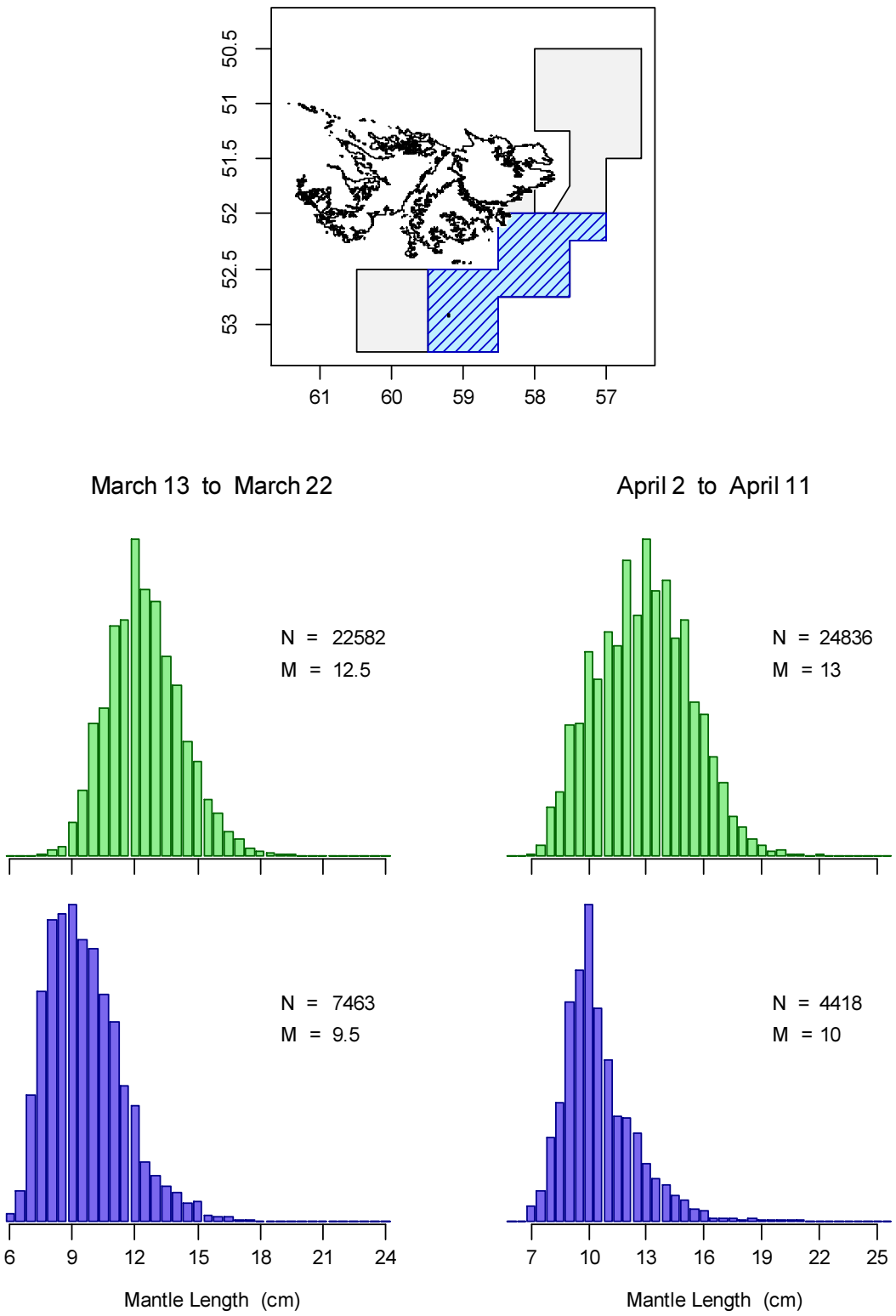

Figure 2. Top: In blue, south sub-area exclusion zone closed to *D. gahi* trawling from March 23rd through March 31st, and from April 12th through April 16th. Below: *D. gahi* mantle length-frequency distributions over the 10 days preceding either closure period; north of 52°S (green) and south of 52°S (purple), with numbers of mantle lengths measured (N) and the median mantle lengths (M cm).

Table 1. *D. gahi* season comparisons since 2004, when catch management was assumed by the FIFD. Days: total number of calendar days open to licensed *D. gahi* fishing including (since 1st season 2013) optional extension days; V-Days: aggregate number of licensed *D. gahi* fishing days reported by all vessels for the season. Entries in italics are seasons closed by emergency order.

	Season 1			Season 2		
	Catch (t)	Days	V-Days	Catch (t)	Days	V-Days
2004	7,152	46	625	17,559	78	1271
2005	24,605	45	576	29,659	78	1210
2006	19,056	50	704	*23,238*	*53*	*883*
2007	17,229	50	680	*24,171*	*63*	*1063*
2008	24,752	51	780	26,996	78	1189
2009	12,764	50	773	*17,836*	*59*	*923*
2010	28,754	50	765	36,993	78	1169
2011	15,271	50	771	*18,725*	*70*	*1099*
2012	34,767	51	770	35,026	78	1095
2013	19,908	53	782	19,614	78	1195
2014	28,119	59	872	19,630	71	1099
2015	*19,383**	*57**	*871**	*10,190*	*42*	*665*
2016	22,616	68	1020	23,089	68	1004
2017	39,433	68	999†	24,101	69	1002‡
2018	43,085	69	975			

* Does not include C-license catch or effort after the C-license target for that season was switched from *D. gahi* to *Illex*.
† Includes two vessel-days of experimental fishing for juvenile toothfish.
‡ Includes one vessel-day of experimental fishing for juvenile toothfish.

Five extraordinary management orders were issued for this season: (1) With reference to pinniped captures in the previous season (Winter 2017b), all vessels were required to embark an observer tasked (at minimum) to monitor the presence and incidental capture of pinnipeds. (2) The Loligo Box south of 52°S and east of 59.5°W was closed from March 23rd through March 31st, because of the small sizes of *D. gahi* reported in the south compared to the north (Figure 2). (3) After a test period of open fishing, the Loligo Box was again closed south of 52°S and east of 59.5°W from April 12th through April 16th, for continuing concern over the small sizes of *D. gahi* in the south (Figure 2). (4) The use of Seal Exclusion Devices (SEDs) was mandated in the north sub-area of the Loligo Box (north of 52° S latitude) from April 26th until the end of the season, following four reported fishing mortalities of Southern sea lions *Otaria flavescens* in the north. (5) The use of SEDs was additionally mandated in the south sub-area of the Loligo Box (south of 52° S latitude) from May 3rd until the end of the season, following two reported fishing mortalities of South American fur seals *Arctocephalus australis* in the south.

Assessment of the Falkland Islands *D. gahi* stock was conducted with depletion time-series models as in previous seasons (Agnew et al. 1998, Roa-Ureta and Arkhipkin 2007; Arkhipkin et al. 2008), and in other squid fisheries (Royer et al. 2002, Young et al. 2004, Chen et al. 2008, Morales-Bojórquez et al. 2008, Keller et al. 2015, Medellín-Ortiz et al. 2016). Because *D. gahi* has an annual life cycle (Patterson 1988, Arkhipkin 1993), stock cannot be derived from a standing biomass carried over from prior years (Rosenberg et al. 1990, Pierce and Guerra 1994). The depletion model instead calculates an estimate of population abundance over time by evaluating what levels of abundance and catchability must be extant to sustain the observed rate of catch. Depletion modelling of the *D. gahi* target

fishery is used both in-season and for the post-season summary, with the objective of maintaining an escapement biomass of 10,000 tonnes *D. gahi* at the end of each season as a conservation threshold (Agnew et al. 2002, Barton 2002).

Methods

The depletion model formulated for the Falklands *D. gahi* stock is based on the equivalence:

$$C_{day} = q \times E_{day} \times N_{day} \times e^{-M/2} \quad \textbf{(1)}$$

where q is the catchability coefficient, M is the natural mortality rate (considered constant at 0.0133 day^{-1}; Roa-Ureta and Arkhipkin 2007), and C_{day}, E_{day}, N_{day} are catch (numbers of squid), fishing effort (numbers of vessels), and abundance (numbers of squid) per day. In its basic form (DeLury 1947) the depletion model assumes a closed population in a fixed area for the duration of the assessment. However, the assumption of a closed population is imperfectly met in the Falkland Islands fishery, where stock analyses have often shown that *D. gahi* groups arrive in successive waves after the start of the season (Roa-Ureta 2012; Winter and Arkhipkin 2015). Arrivals of successive groups are inferred from discontinuities in the catch data. Fishing on a single, closed cohort would be expected to yield gradually decreasing CPUE, but gradually increasing average individual sizes, as the squid grow. When instead these data change suddenly, or in contrast to expectation, the immigration of a new group to the population is indicated (Winter and Arkhipkin 2015).

In the event of a new group arrival, the depletion calculation must be modified to account for this influx. This is done using a simultaneous algorithm that adds new arrivals on top of the stock previously present, and posits a common catchability coefficient for the entire depletion time-series. If two depletions are included in the same model (i.e., the stock present from the start plus a new group arrival), then:

$$C_{day} = q \times E_{day} \times (N1_{day} + (N2_{day} \times i2|_0^1)) \times e^{-M/2} \quad \textbf{(2)}$$

where i2 is a dummy variable taking the values 0 or 1 if 'day' is before or after the start day of the second depletion. For more than two depletions, $N3_{day}$, i3, $N4_{day}$, i4, etc., would be included following the same pattern.

Because SEDs were mandated towards the end of this season, the SED modification of the depletion model developed last year (Winter 2017b) was implemented again for this season's assessment:

$$\begin{aligned} C_{day} &= q_{SED} \times E_{SED\text{-}day} \times (N1_{day} + (N2_{day} \times i2|_0^1)) \times e^{-M/2} \\ &+ q_{NSED} \times E_{NSED\text{-}day} \times (N1_{day} + (N2_{day} \times i2|_0^1)) \times e^{-M/2} \end{aligned} \quad \textbf{(3)}$$

whereby the depletion catch equation **2** is formulated as the composite of fishing effort in parallel with and without SEDs (subscripts SED and NSED). The process of SEDs differed in this season as all vessels were mandated simultaneously to start fishing with SEDs on the same day; i.e., implementation was not individual in the same way as last season. The structure of the model is nevertheless the same (Equation **3**); it simply means that either $E_{SED\text{-}day}$ or $E_{NSED\text{-}day} = 0$ on any given day. As before, the computational difference between q_{SED} and q_{NSED} includes not only the technical efficacy of either gear but all fishing aspects

that correlate with the gear; e.g., that vessels fishing under SED 'conditions' might also be taking shorter trawls than otherwise, or switching locations more frequently or distantly.

The season depletion likelihood function was calculated as the difference between actual catch numbers reported and catch numbers predicted from the model (Equation **3**), statistically corrected by a factor relating to the number of days of the depletion period (Roa-Ureta, 2012):

$$((n\text{Days} - 2)/2) \times \log\left(\sum_{days} \left(\log(\text{predicted C}_{\text{day}}) - \log(\text{actual C}_{\text{day}})\right)^2 \right) \quad \textbf{(4)}$$

The stock assessment was set in a Bayesian framework (Punt and Hilborn 1997), whereby results of the season depletion model are conditioned by prior information on the stock; in this case the information from the pre-season survey.

The likelihood function of prior information was calculated as the normal distribution of the difference between catchability (q) derived from the survey abundance estimate, and catchability derived from the season depletion model. Applying this difference requires both the survey and the season to be fishing the same stock with the same gear (Winter et al. 2018). Catchability, rather than abundance N, is used for calculating prior likelihood because catchability informs the entire season time series; whereas N from the survey only informs the first in-season depletion period – subsequent immigrations and depletions are independent of the abundance that was present during the survey. In this season, only NSED fishing was conducted in the pre-season survey (Winter et al. 2018), and therefore only q_{NSED} could be linked to a prior. Thus, the prior likelihood function was:

$$\frac{1}{\sqrt{2\pi \cdot \text{SD}_{\text{q prior NSED}}^{\ 2}}} \times \exp\left(- \frac{\left(q_{\text{model NSED}} - q_{\text{prior NSED}}\right)^2}{2 \cdot \text{SD}_{\text{q prior NSED}}^{\ 2}} \right) \quad \textbf{(5)}$$

where the standard deviation of catchability prior ($SD_{\text{q prior NSED}}$) was calculated from the Euclidean sum of the survey prior estimate uncertainty, the variability in catches on the season start date, and the uncertainty in the natural mortality M estimate over the number of days mortality discounting (Appendix: Equations **A5-C**, **A5-S**).

Bayesian optimization of the depletion was calculated by jointly minimizing Equations **4** and **5**, using the Nelder-Mead algorithm in R programming package 'optimx' (Nash and Varadhan 2011). Relative weights in the joint optimization were assigned to Equations **4** and **5** as the converse of their coefficients of variation (CV), i.e., the CV of the prior became the weight of the depletion model and the CV of the depletion model became the weight of the prior. Calculations of the CVs are described in Equations **A8-N** and **A8-S**. Because a complex model with multiple depletions may converge on a local minimum rather than global minimum, the optimization was stabilized by running a feed-back loop that set the q and N parameter outputs of the Bayesian joint optimization back into the in-season-only minimization (Equation **4**), re-calculated this minimization and the CV resulting from it, then re-calculated the Bayesian joint optimization, and continued this process until both the in-season minimization and the joint optimization remained unchanged.

With actual C_{day}, $E_{\text{NSED - day}}$, $E_{\text{SED - day}}$, and M being fixed parameters, the optimization of Equation **3** using **4** and **5** produces estimates of q_{NSED}, q_{SED}, and N1, N2, …, etc. Numbers of squid on the final day (or any other day) of a time series are then calculated as the numbers N of the depletion start days discounted for natural mortality during the

intervening period, and subtracting cumulative catch also discounted for natural mortality (CNMD). Taking for example a two-depletion period:

$$\begin{aligned} N_{\text{final day}} &= N1_{\text{start day 1}} \times e^{-M\,(\text{final day} - \text{start day 1})} \\ &+ N2_{\text{start day 2}} \times e^{-M\,(\text{final day} - \text{start day 2})} \\ &- CNMD_{\text{final day}} \end{aligned} \quad \textbf{(6)}$$

where

$$\begin{aligned} CNMD_{\text{day 1}} &= 0 \\ CNMD_{\text{day x}} &= CNMD_{\text{day x-1}} \times e^{-M} + C_{\text{day x-1}} \times e^{-M/2} \end{aligned} \quad \textbf{(7)}$$

$N_{\text{final day}}$ is then multiplied by the average individual weight of squid on the final day to give biomass. Daily average individual weight is obtained from length / weight conversion of mantle lengths measured in-season by observers, and also derived from in-season commercial data as the proportion of product weight that vessels reported per market size category. Observer mantle lengths are scientifically accurate, but restricted to 1-2 vessels at any one time that may or may not be representative of the entire fleet, and not available every day. Commercially proportioned mantle lengths are relatively less accurate, but cover the entire fishing fleet every day. Therefore, both sources of data are used (see Appendix – *Doryteuthis gahi* individual weights).

Distributions of the likelihood estimates from joint optimization (i.e., measures of their statistical uncertainty) were computed using a Markov Chain Monte Carlo (MCMC) (Gamerman and Lopes 2006), a method that is commonly employed for fisheries assessments (Magnusson et al. 2013). MCMC is an iterative process which generates random stepwise changes to the proposed outcome of a model (in this case, the q and N of *D. gahi* squid) and at each step, accepts or nullifies the change with a probability equivalent to how well the change fits the model parameters compared to the previous step. The resulting sequence of accepted or nullified changes (i.e., the 'chain') approximates the likelihood distribution of the model outcome. The MCMC of the depletion models were run for 200,000 iterations; the first 1000 iterations were discarded as burn-in sections (initial phases over which the algorithm stabilizes); and the chains were thinned by a factor equivalent to the maximum of either 5 or the inverse of the acceptance rate (e.g., if the acceptance rate was 12.5%, then every 8^{th} (0.125^{-1}) iteration was retained) to reduce serial correlation. For each model three chains were run; one chain initiated with the parameter values obtained from the joint optimization of Equations **4** and **5**, one chain initiated with these parameters ×2, and one chain initiated with these parameters ×¼. Convergence of the three chains was accepted if the variance among chains was less than 10% higher than the variance within chains (Brooks and Gelman 1998). When convergence was satisfied the three chains were combined as one final set. Equations **6**, **7**, and the multiplication by average individual weight were applied to the CNMD and each iteration of N values in the final set, and the biomass outcomes from these calculations represent the distribution of the estimate. The peaks of the MCMC histograms were compared to the empirical optimizations of the N values.

Depletion models and likelihood distributions were calculated separately for north and south sub-areas of the Loligo Box fishing zone, as *D. gahi* sub-stocks emigrate from different spawning grounds and remain to an extent segregated (Arkhipkin and Middleton 2002). Total escapement biomass is then defined as the aggregate biomass of *D. gahi* on the last day of the season for north and south sub-areas combined. North and south biomasses are not assumed to be uncorrelated however (Shaw et al. 2004), and therefore north and south likelihood distributions were added semi-randomly in proportion to the strength of their day-to-day correlation (see Winter 2014, for the semi-randomization algorithm).

Stock assessment
Data

The fishery in this season showed an unusual level of disconnect from the pre-season survey. The pre-season survey estimated only 569 t *D. gahi* biomass (1.8%) in the north sub-area vs. 31,625 t *D. gahi* biomass (8.2%) in the south sub-area (Winter et al. 2018). In-season, 32,367 t (75.1%) were caught in the north sub-area vs. 10,718 t (24.9%) caught in the south sub-area, with 69.2% of vessel-days taken in the north sub-area and 30.8% of vessel-days in the south sub-area. The imbalance (Figures 3, 4) is partially due to closures in the south, but underscores that most *D. gahi* biomass in the north supplying this exceptionally high catch season arrived only after the end of the survey. As a result, survey abundance in the north was poorly suited as a prior (cf. Equation **5**) for the north sub-area depletion model. Instead, the prior was set by averaging catchability of the north + south abundance (**A4-C**, **A5-C**). This adaptation reflects the principle of 'borrowing' information from compatible data sets (Su et al. 2001, Jiao et al 2011), that was similarly used for the 1st season 2017 stock assessment (Winter 2017a).

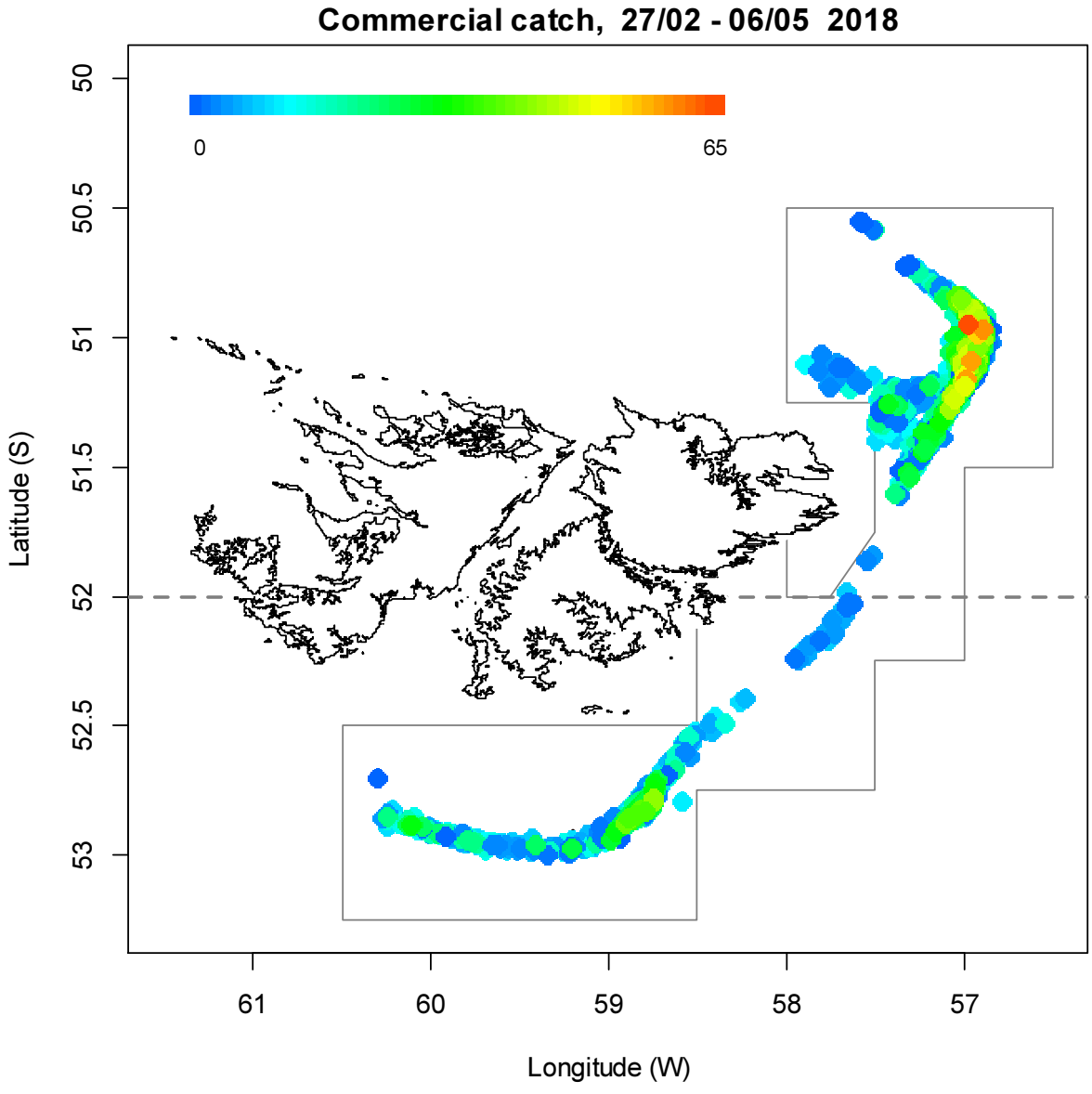

Figure 3 [previous page]. Spatial distribution of *D. gahi* 1st-season trawls, colour-scaled to catch weight (maximum = 65.0 tonnes). 3078 trawl catches were taken during the season. The 'Loligo Box' fishing zone, as well as the 52 ºS parallel delineating the boundary between north and south assessment sub-areas, are shown in grey.

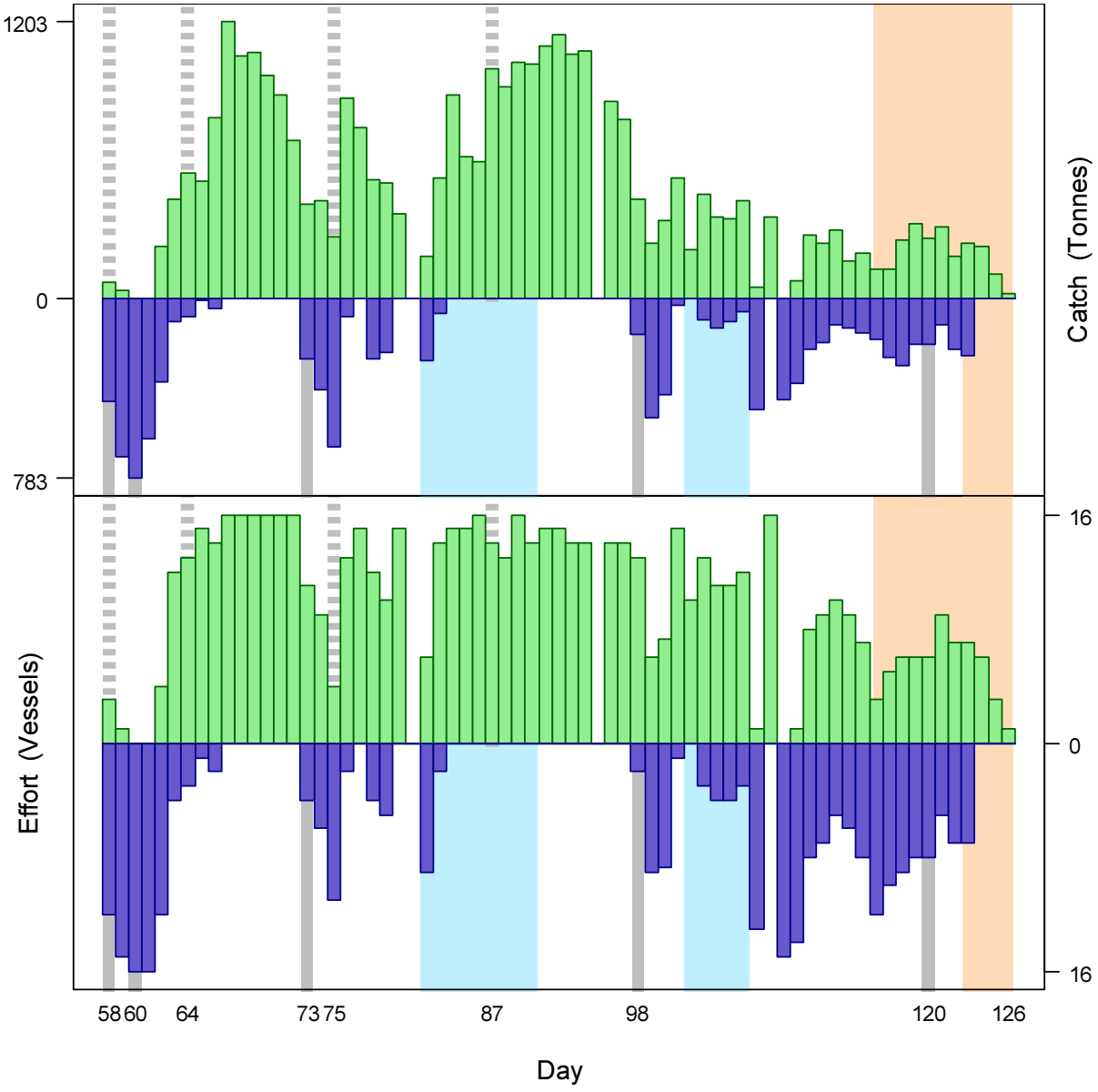

Figure 4. Daily total *D. gahi* catch and effort distribution by assessment sub-area north (green) and south (purple) of the 52º S parallel during 1st season 2018. The season was open from February 27th (chronological day 58) to May 1st (chronological day 121), plus flex days until May 6th (day 126). Blue under-shading delineates the partial closure periods in the south sub-area of the Loligo Box; orange under-shading delineates the mandatory use of SEDs north and south. As many as 16 vessels fished per day north; as many as 16 vessels fished per day south. As much as 1203 tonnes *D. gahi* was caught per day north; as much as 783 tonnes *D. gahi* was caught per day south.

975 vessel-days were fished during the season (Table 1), with a median of 15 vessels per day (mean 14.6) except for flex and weather extensions. Vessels reported daily catch totals to the FIFD and electronic logbook data that included trawl times, positions, depths, and product weight by market size categories. Three FIG fishery observers were deployed on five vessels in the fishing season for a total of 54 observer-days (Chemshirova 2018, Iriarte 2018a; 2018b, Trevizan 2018a; 2018b). Throughout the 69 days of the season, 22 days had no FIG fishery observer covering (including 3 of the 5 season-end extension days), 40 days had 1 FIG fishery observer covering, and 7 days had two FIG fishery observers covering. The FIG seabird observer was deployed for 13 days on two vessels during the season (Kuepfer 2018a; 2018b). The protocol for seabird observation by FIG fishery observers was amended this season to match the finfish fishery: one day of bird observation every fourth day. On other days FIG fishery observers were tasked as usual with sampling 200 *D. gahi* at two stations; reporting their maturity stages, sex, and lengths to 0.5 cm. Contract marine mammal monitors were tasked with measuring 200 unsexed lengths of *D. gahi* per day. The length-weight relationship for converting observer and commercially proportioned lengths was combined from 1st pre-season and season data of both 2017 and 2018, as 2018 data became available progressively. The final parameterization of the length-weight relationship included 2063 measures from 2017 and 1510 measures from 2018, giving:

$$\text{weight (kg)} = 0.218 \times \text{length (cm)}^{2.140} / 1000 \quad \textbf{(8)}$$

with a coefficient of determination $R^2 = 92.4\%$.

Group arrivals / depletion criteria

Start days of depletions - following arrivals of new *D. gahi* groups - were judged primarily by daily changes in CPUE, with additional information from sex proportions, maturity, and average individual squid sizes. CPUE was calculated as metric tonnes of *D. gahi* caught per vessel per day. Days were used rather than trawl hours as the basic unit of effort. Commercial vessels do not trawl standardized duration hours, but rather durations that best suit their daily processing requirements. An effort index of days is therefore more consistent.

Four days in the north and five days in the south were identified that represented the onset of separate immigrations / depletions throughout the season.

- The first depletion north was set on day 58 (February 27th), the first day of fishing in the north sub-area (by three vessels). Average commercial weight and observer weight were close to the lowest before the mid-point of the season (Figure 5A and B).
- The second depletion north was identified on day 64 (March 5th) with a small increase in CPUE (Figure 6) and local minima in average commercial weight, average observer weight, and maturity (Figure 5A, B, and D).
- The third depletion north was identified on day 75 (March 16th) with a sharp increase to the highest CPUE in seven days (Figure 6).
- The fourth depletion north was identified on day 87 (March 28th), when average commercial weights reached its highest peak before decreasing towards the end of the season; conversely average observer weight and maturity suggested local minima (Figure 5A, B, and D), and CPUE increased sharply to the highest level in 20 days (Figure 6).
- The first depletion south was set on day 58 (February 27th), the first day of fishing in the south sub-area (by twelve vessels). Average observer weight and average maturity were close to the lowest before the mid-point of the season (Figure 5A and D).

- The second depletion south was identified only two days later on day 60 (March 1st), when average observer weight and average maturity remained low (Figure 5A and D) and CPUE increased to the highest level for the next two weeks (Figure 6).
- The third depletion south was identified on day 73 (March 14th) when average commercial weight underwent a small decrease (Figure 5A) and CPUE reached its highest peak up to that point in the season (Figure 6).
- The fourth depletion south was set on day 98 (April 8th) when fishing resumed in the south after a hiatus of 15 days, and two vessels achieved the highest CPUE of the season (Figure 6).
- The fifth depletion south was identified on day 120 (April 30th) when average commercial and observer weights showed local minima (Figure 5A and B) and the proportion of females started decreasing precipitously the day after (Figure 5C).

Figure 5 [below]. A: Average individual *D. gahi* weights (kg) per day from commercial size categories. B: Average individual *D. gahi* weights (kg) by sex per day from observer sampling. C: Proportions of female *D. gahi* per day from observer sampling. D: Average maturity value by sex per day from observer sampling. In all graphs – Males: triangles, females: squares, unsexed: circles. North sub-area: green, south sub-area: purple. Data from consecutive days are joined by line segments. Broken grey bars indicate the starts of in-season depletions north. Solid grey bars indicate the starts of in-season depletions south.

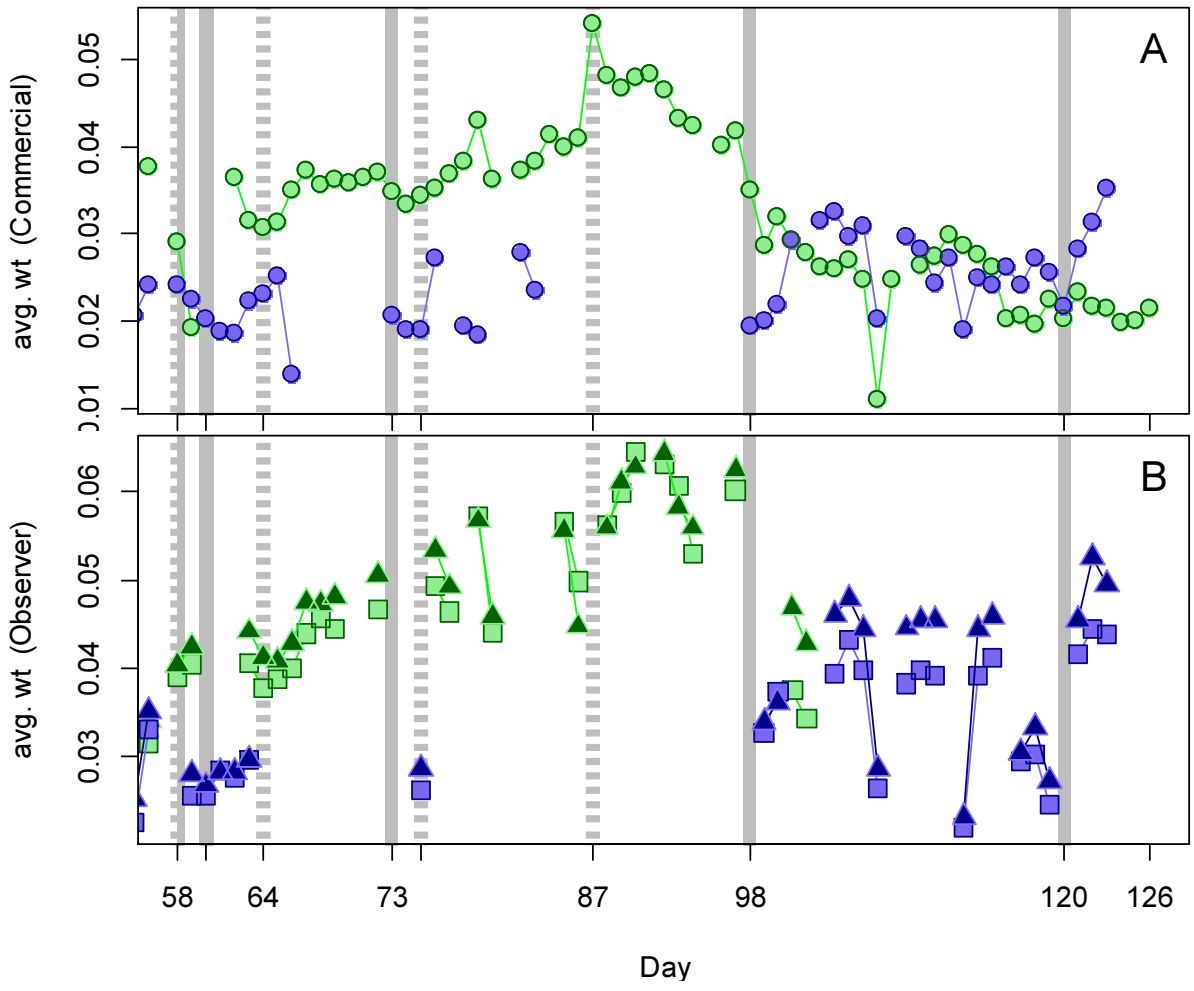

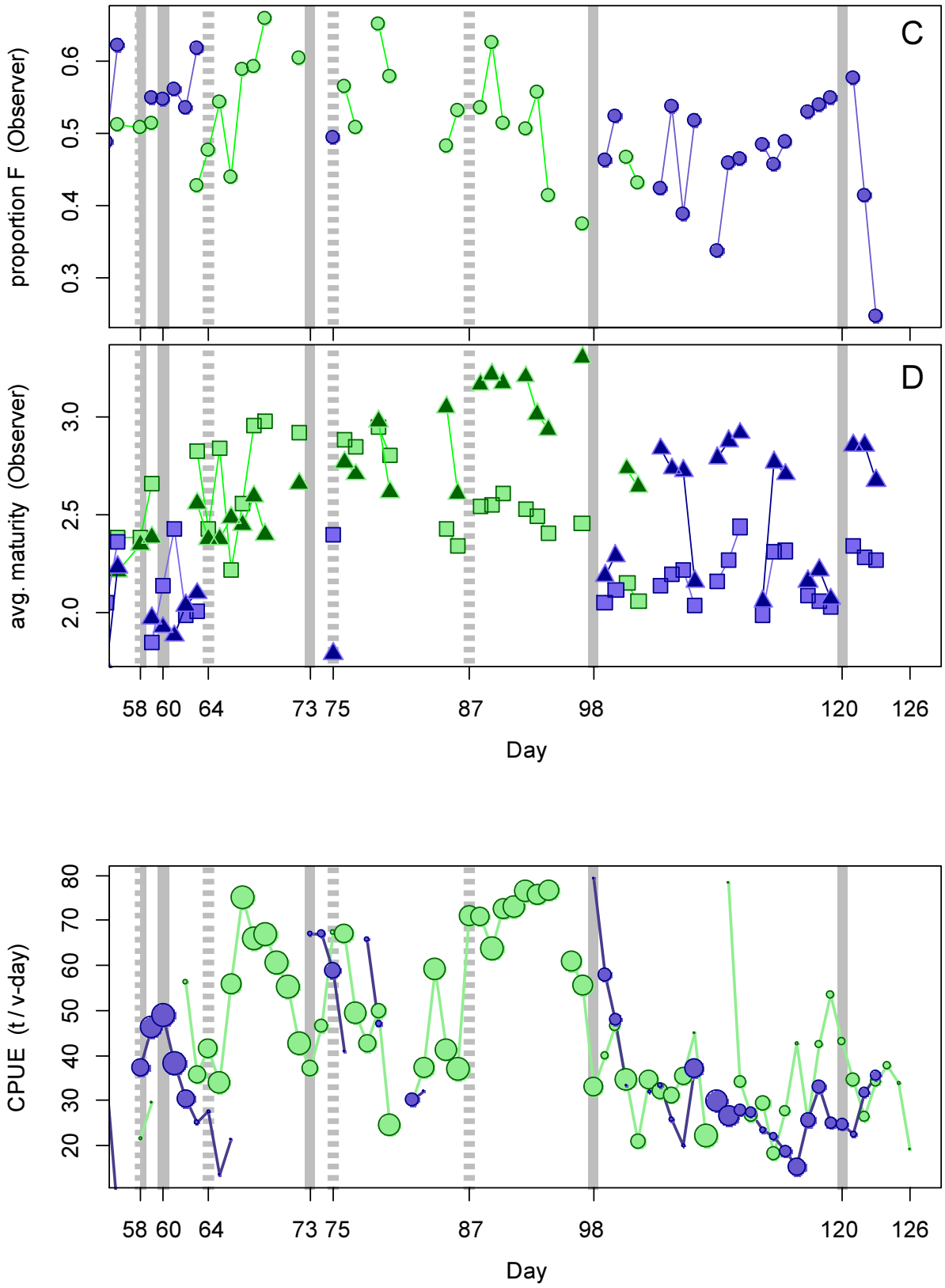

Figure 6. CPUE in metric tonnes per vessel per day, by assessment sub-area north (green) and south (purple) of 52° S latitude. Circle sizes are proportioned to numbers of vessels fishing. Data from consecutive days are joined by line segments. Broken grey bars indicate the starts of in-season depletions north. Solid grey bars indicate the starts of in-season depletions south.

Depletion analyses
North

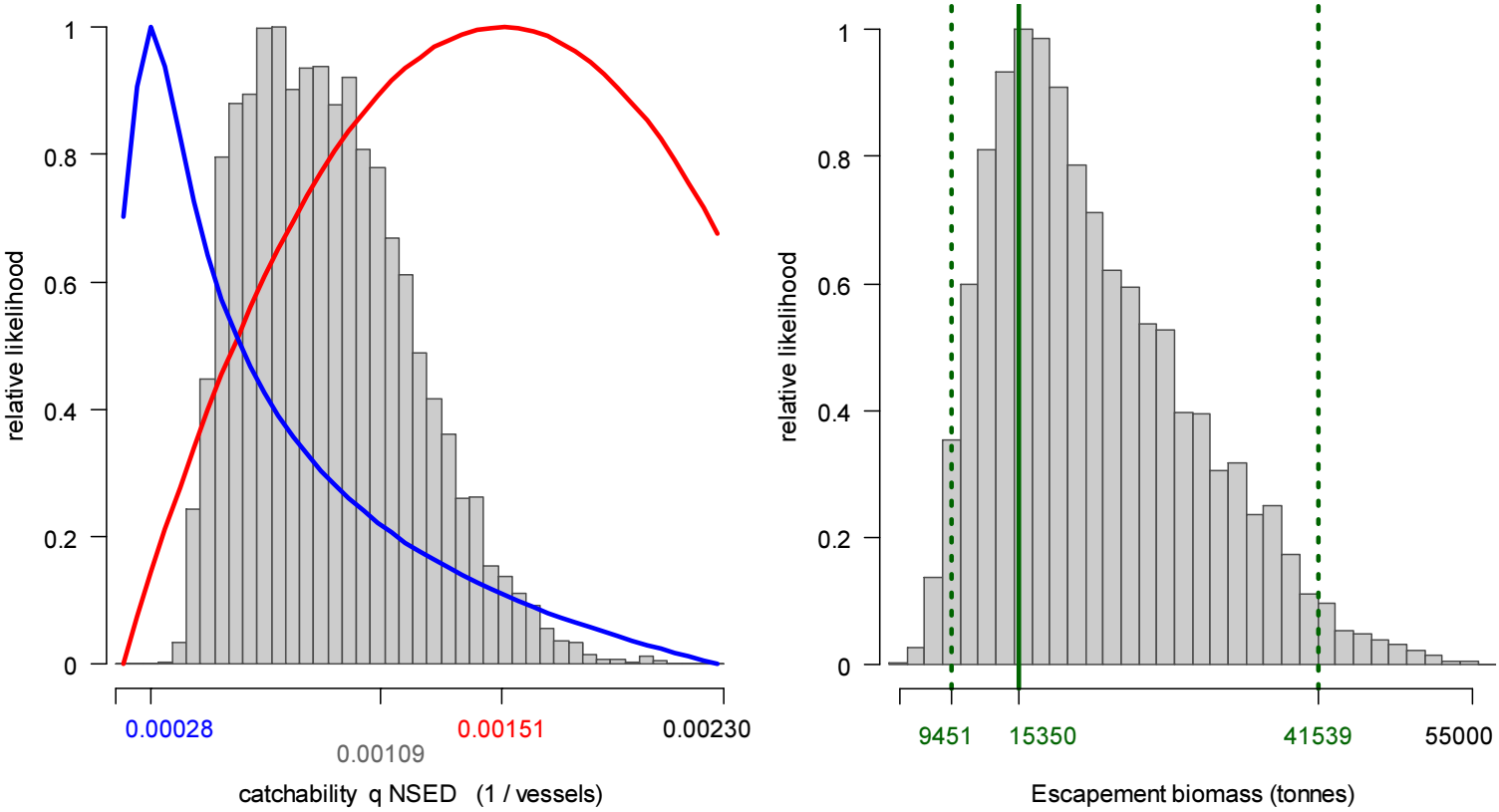

Figure 7. North sub-area. Left: Likelihood distributions for *D. gahi* NSED catchability. Red line: prior model (pre-season survey data), blue line: in-season depletion model, grey bars: combined Bayesian model posterior. Right: Likelihood distribution (grey bars) of escapement biomass, from Bayesian posterior and average individual squid weight at the end of the season. Green lines: maximum likelihood and 95% confidence interval. Note the correspondence to Figure 8.

In the north sub-area, Bayesian optimization on catchability (q) without SEDs resulted in a maximum likelihood posterior of $_{\text{Bayesian}}\, q_{\text{N NSED}} = 1.086 \times 10^{-3}$ (Figure 7, left, and Equation **A9-N**). The pre-season prior was higher at $_{\text{prior}}\, q_{\text{C}} = 1.514 \times 10^{-3}$; Figure 7, left, and Equation **A4-C**), while in-season depletion optimized lower with a sharp peak at $_{\text{depletion}}\, q_{\text{N NSED}} = 0.277 \times 10^{-3}$ (Figure 7, left, and **A6-N**). Bayesian optimization was weighted as 0.935 for in-season depletion (**A5-C**) vs. 0.366 for the prior (**A8-N**). Depletion model estimation showed a relatively diffuse distribution (i.e., the 'ragged' appearance of grey bar plots in Figure 7 left and right). The distribution may be due in particular to the second depletion – on day 64 – being inferred three days before CPUE responded with a major peak (Figure 6). On day 64, all 13 vessels fishing north reported their noon position in either grid XNAP or XPAP; on day 67 fourteen of 16 vessels fishing north reported their noon position in XMAQ or XNAQ, suggesting that the fleet had not immediately located the higher abundance of squid. As a result, the depletion model fit the time-series data poorer than usual.

Posterior catchability with SEDs was $_{\text{Bayesian}}\, q_{\text{N SED}} = 1.902 \times 10^{-3}$ (Equation **A9-N**). As occurred during 2nd season 2017 (Winter 2017), this implies that fishing in the north with

a SED in the net had higher squid catch efficacy than fishing without a SED: 1.902×10^{-3} / $1.086 \times 10^{-3} = 175.17\%$. Again as in 2nd season 2017, this may however be due to the course of the fishery rather than actual characteristics of the net. After SEDs were mandated in the north starting April 26th, a greater proportion of vessels moved to fish south than previously on average during the season (Figure 4). Furthermore, as a depletion model is inherently predisposed to realize decreasing abundance over time, catchability, defined as catch per effort per abundance (Arreguín-Sánchez 1996), may be biased to higher values as the season progresses. Thus, q_{NSED} vs. q_{SED} should continue to be seen as an arbitrary difference between two types of fishing gear.

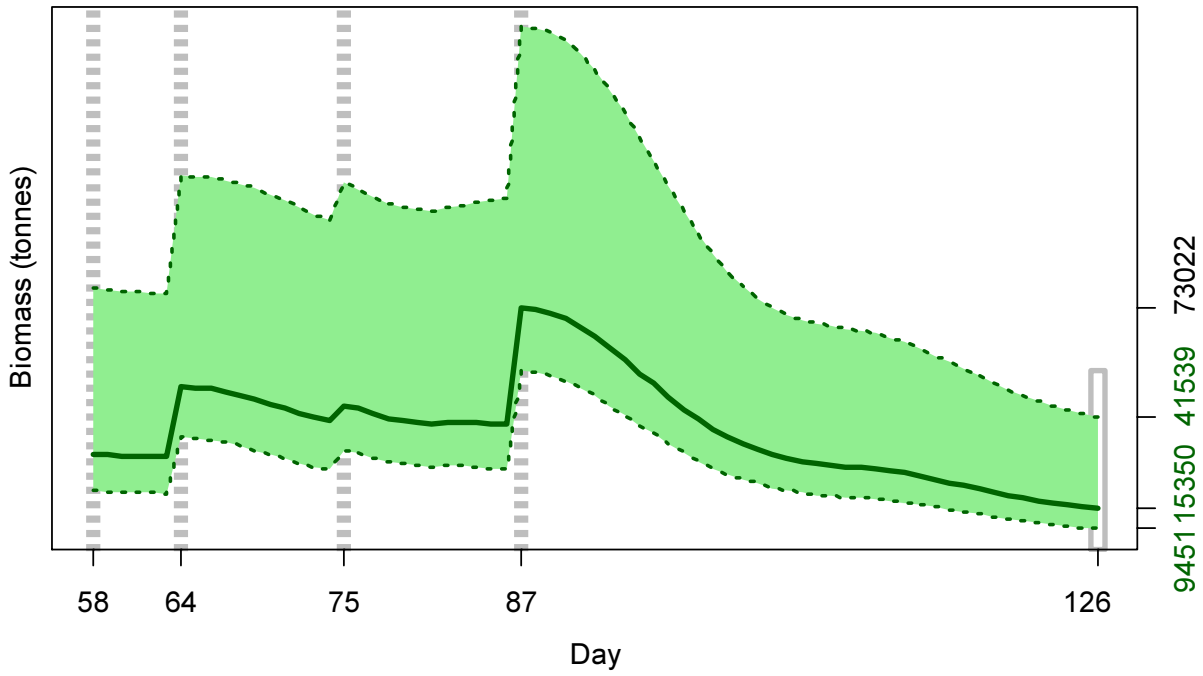

Figure 8. North sub-area. *D. gahi* biomass time series estimated from Bayesian posterior of the depletion model ± 95% confidence intervals. Broken grey bars indicate the start of in-season depletions north; days 58, 64, 75 and 87. Note that the biomass 'footprint' on day 126 (May 6th) corresponds to the right-side plot of Figure 7.

The MCMC distribution of the Bayesian posterior multiplied by the GAM fit of average individual squid weight (Figure A1-north) gave the likelihood distribution of *D. gahi* biomass on day 126 (May 6th) shown in Figure 7-right, with maximum likelihood and 95% confidence interval of:

$$B_{N\ day\ 126} = 15{,}350\ t \sim 95\%\ CI\ [9{,}451 - 41{,}539]\ t \quad \textbf{(9)}$$

At its highest point (fourth depletion start: day 87 – March 28th), estimated *D. gahi* biomass north was 73,022 t ~ 95% CI [54,915 – 153,405] t (Figure 8). Notably, average individual sizes of *D. gahi* decreased steadily after day 87 (Figure 5A, and to a lesser extent 5B), indicative that immigration continued at a slow trickle and contributing to the high abundance of the season.

South

In the south sub-area, Bayesian optimization on catchability q without SEDs resulted in a maximum likelihood posterior ($_{\text{Bayesian}}\ q_{\ S\ NSED} = 1.737 \times 10^{-3}$; Figure 9, left, and Equation **A9-S**) that was slightly higher than the pre-season prior ($_{\text{prior}}\ q_{\ S} = 1.370 \times 10^{-3}$; Figure 9, left, and Equation **A4-S**), while the in-season depletion was higher than the maximum of the MCMC distribution at $_{\text{depletion}}\ q_{\ S\ NSED} = 3.844 \times 10^{-3}$ (Figure 9, left, and **A6-S**). Bayesian optimization was weighted as the converse of the CVs: 0.932 for in-season depletion (**A5-S**) vs. 0.477 for the prior (**A8-S**). Despite the in-season depletion q being weighted nearly twice as high as the prior, it evidently imposed little selectivity on the model (Figure 9, left).

Posterior catchability with SEDs was $_{\text{Bayesian}}\ q_{\ S\ SED} = 2.335 \times 10^{-3}$ (Equation **A9-S**). As only 7 vessel-days of effort were taken in the south after the SED mandate starting May 3rd (all on May 3rd), the SED factor brought little importance to the model.

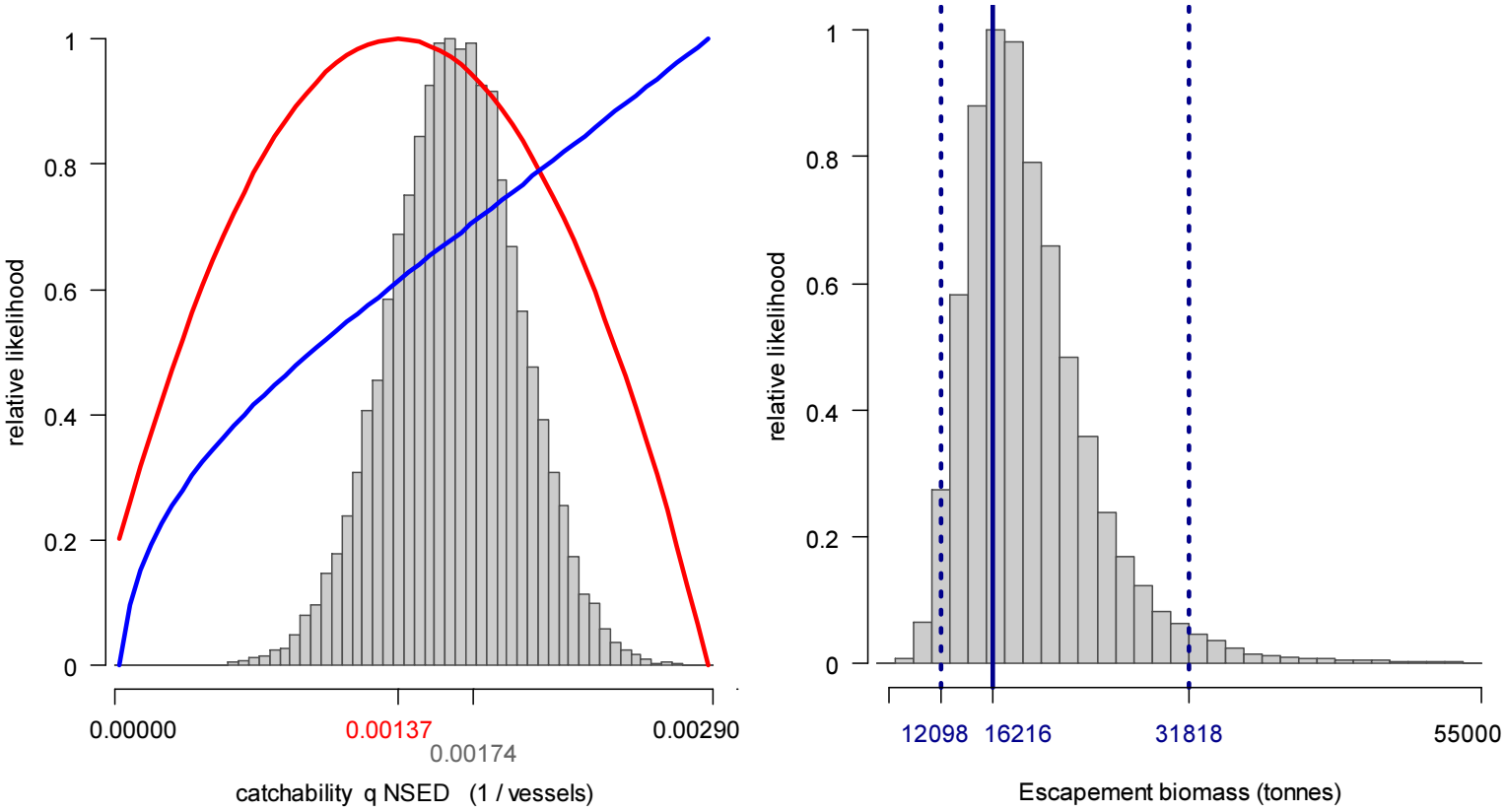

Figure 9. South sub-area. Left: Likelihood distributions for *D. gahi* NSED catchability. Red line: prior model (pre-season survey data), blue line: in-season depletion model, grey bars: combined Bayesian model posterior. Right: Likelihood distribution (grey bars) of escapement biomass, from Bayesian posterior and average individual squid weight at the end of the season. Blue lines: maximum likelihood and 95% confidence interval. Note correspondence to Figure 10.

Figure 10 [next page]. South sub-area. *D. gahi* biomass time series estimated from Bayesian posterior of the depletion model ± 95% confidence intervals. Grey bars indicate the start of in-season depletions south; days 58, 60, 73, 98 and 120. Note that the biomass 'footprint' on day 126 (May 6th) corresponds to the right-side plot of Figure 9.

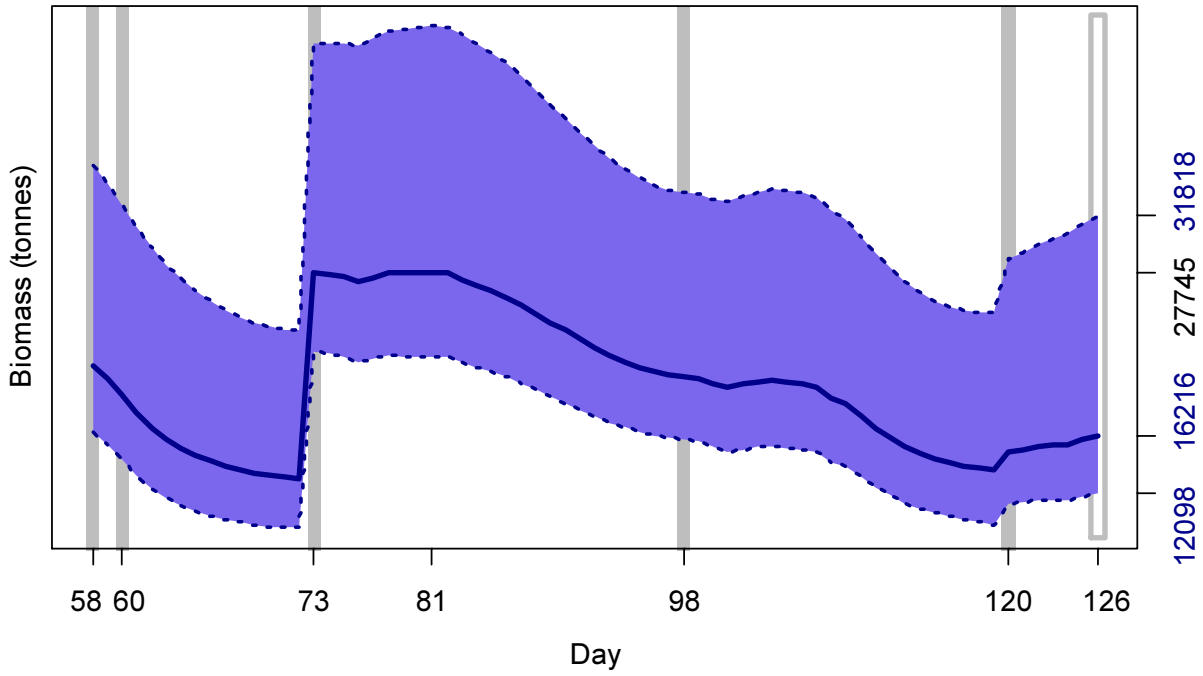

The MCMC distribution of the Bayesian posterior multiplied by the GAM fit of average individual squid weight (Figure A1-south) gave the likelihood distribution of *D. gahi* biomass on day 126 (May 6th) shown in Figure 9-right, with maximum likelihood and 95% confidence interval of:

$$B_{S\ day\ 126} = 16{,}216\ t \sim 95\%\ CI\ [12{,}098 - 31{,}818]\ t \quad \textbf{(10)}$$

At its highest point (day 81; March 22nd), estimated *D. gahi* biomass south was 27,745 t ~ 95% CI [21,768 – 45,196] t (Figure 10). March 22nd was one of two bad-weather days when no fishing at all occurred in the Loligo Box (Figure 1), and followed a period of low effort in the south (Figure 4). Thus, natural mortality alone did not outweigh the growth of squid, and biomass increased slightly from the previous immigration on day 73 (Figure 10). Similarly, biomass increased after the last immigration on day 120, as effort was low from then (Figure 4) and individual sizes showed a strong average increase (Figure 5A and B). Two immigration / depletion days, 60 and 98, showed almost no inflection on the biomass time series (Figure 10 and Equation **A9-S**). A test run of the depletion model confirmed that the biomass time series would have been practically identical modelled on just three immigration days (58, 73 and 120) excluding 60 and 98 (data not shown). Thus, immigration events that may have been misspecified did not distort the model.

Escapement biomass

Total escapement biomass was defined as the aggregate biomass of *D. gahi* at the end of day 126 (May 6th) for north and south sub-areas combined (Equations **9** and **10**). Depletion models are calculated on the inference that all fishing and natural mortality are gathered at mid-day, thus a half day of mortality ($e^{-M/2}$) was added to correspond to the closure of the fishery at 23:59 (mid-night) on May 6th for the final remaining vessel: Equation **11**. Semi-randomized addition of the north and south biomass estimates gave the aggregate likelihood

distribution of total escapement biomass shown in Figure 11. North and south biomass time series had comparatively low correlation (R = 0.444), resulting in a maximum likelihood that was not precisely centred on the aggregate distribution.

$$B_{\text{Total day 126}} = (B_{\text{N day 126}} + B_{\text{S day 126}}) \times e^{-M/2}$$

$$= 31{,}566 \text{ t} \times 0.9934$$

$$= 31{,}356 \text{ t} \sim 95\% \text{ CI } [24{,}140 - 65{,}208] \text{ t} \quad \textbf{(11)}$$

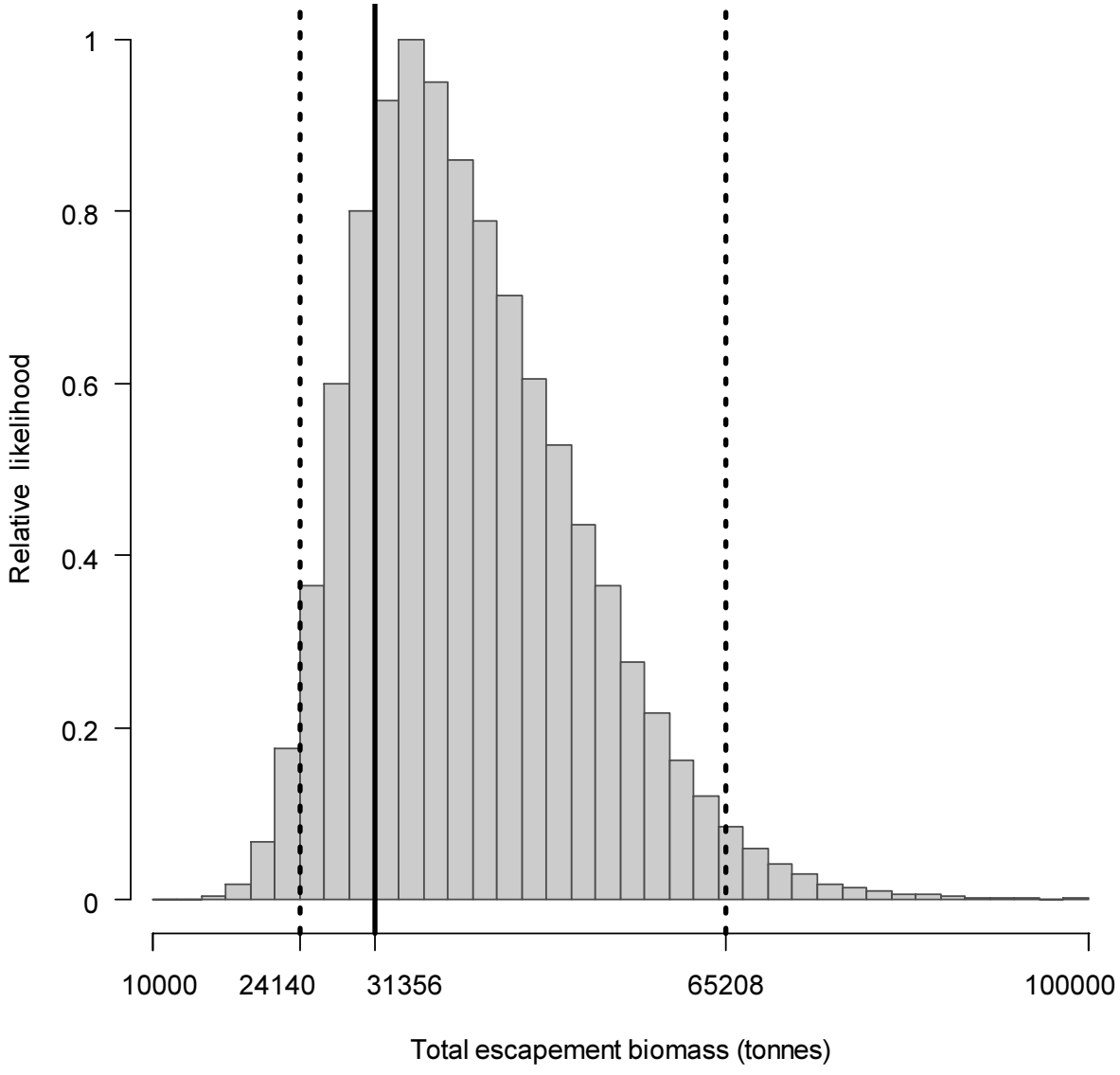

Figure 11. Likelihood distribution with 95% confidence intervals of total *D. gahi* escapement biomass at the season end (May 6th).

The risk of the fishery in the current season, defined as the proportion of the total escapement biomass distribution below the conservation limit of 10,000 tonnes (Agnew et al., 2002; Barton, 2002), was calculated as effectively zero.

The escapement biomass total of 31,356 tonnes was substantially lower than last year (Winter 2017a), but above median of the past five and the past ten 1st seasons. Among 1st seasons since 2005, season catch is significantly positive predictive of escapement biomass (generalized additive model, $p < 0.05$, $R^2 = 0.637$).

Immigration

Doryteuthis gahi immigration during the season was inferred on each day by how many more squid were estimated present than the day before, minus the number caught and the number expected to have died naturally:

$$_{\text{Immigration}}N_{\text{day i}} = N_{\text{day i}} - (N_{\text{day i-1}} - C_{\text{day i-1}} - M_{\text{day i-1}})$$

where $N_{\text{day i-1}}$ are optimized in the depletion models, $C_{\text{day i-1}}$ calculated as in Equation **3**, and $M_{\text{day i-1}}$ is:

$$M_{\text{day i-1}} = (N_{\text{day i-1}} - C_{\text{day i-1}}) \times (1 - e^{-M})$$

Immigration biomass per day was then calculated as the immigration number per day multiplied by predicted average individual weight from the GAM:

$$_{\text{Immigration}}B_{\text{day i}} = {}_{\text{Immigration}}N_{\text{day i}} \times {}_{\text{GAM}}Wt_{\text{day i}}$$

All numbers N are themselves derived from the daily average individual weights, therefore the estimation automatically factors in that those squid immigrating on a given day would likely be smaller than average (because younger). Confidence intervals of the immigration estimates were calculated by applying the above algorithms to the MCMC iterations of the depletion models. Resulting total biomasses of *D. gahi* immigration north and south, up to season end (day 126), were:

$$_{\text{Immigration}}B_{\text{N season}} = 59{,}278 \text{ t} \sim 95\% \text{ CI } [44{,}238 – 105{,}334] \text{ t} \quad \textbf{(12-N)}$$

$$_{\text{Immigration}}B_{\text{S season}} = 14{,}765 \text{ t} \sim 95\% \text{ CI } [11{,}393 – 024{,}490] \text{ t} \quad \textbf{(12-S)}$$

Total immigration with semi-randomized addition of the confidence intervals was:

$$_{\text{Immigration}}B_{\text{Total season}} = 74{,}043 \text{ t} \sim 95\% \text{ CI } [58{,}689 – 124{,}487] \text{ t} \quad \textbf{(12-T)}$$

In the north sub-area, the in-season peaks on days 64, 75, and 87 accounted for approximately 33.3%, 8.9%, and 54.2% of in-season immigration (start day 58 was de facto not an in-season immigration), consistent with the variation in time series biomass on Figure 8. In the south sub-area, the in-season peaks on days 73 and 120 accounted for approximately 88.6% and 7.5% of in-season immigration (Figure 10).

Pinniped bycatch

Pinniped bycatch during 1st season 2018 totalled 6 reported fishing mortalities, distributed as summarized in Table 2. No vessel reported more than a single pinniped mortality. Given the

small number of mortalities and lack of aggregation, statistical analyses of the pinniped mortality distributions were not applicable. No pinniped fishing mortalities were reported after the use of SEDs was mandated starting April 26th in the north, and May 3rd in the south.

Table 2. Reported fishing mortalities of pinnipeds in 1st season 2018.

Date	Species	Grid at haul
March 4th	Southern sea lion	XPAP
April 9th	Southern sea lion	XNAQ
April 22nd	Southern sea lion	XNAQ
April 24th	Southern sea lion	XNAP
May 1st	South American fur seal	XVAL
May 2nd	South American fur seal	XVAL

Fishery bycatch

Of the 975 1st season vessel-days (Table 1), 51 vessel-days reported a primary catch of jellyfish (Medusae) rather than *D. gahi* squid, and one vessel-day reported a primary catch of 51.8% lobster krill (*Munida* spp.) vs. 48.1% *D. gahi*. The jellyfish total of 6463 tonnes, from 772 vessel-days (Table A1), was the highest for any *D. gahi* season since consistent reporting of MED bycatch started in 2007. High jellyfish bycatches occurred in the north (Figure 12), and were notably associated with the weather: 45.5% of the jellyfish bycatch total was taken within 48 hours of one of the four bad-weather days described in Figure 1. The lobster krill bycatch (195.5 tonnes from 160 vessel-days, Table A1) was the highest for a *D. gahi* season since 1st season 2007, and occurred in the south-west (Figure 12).

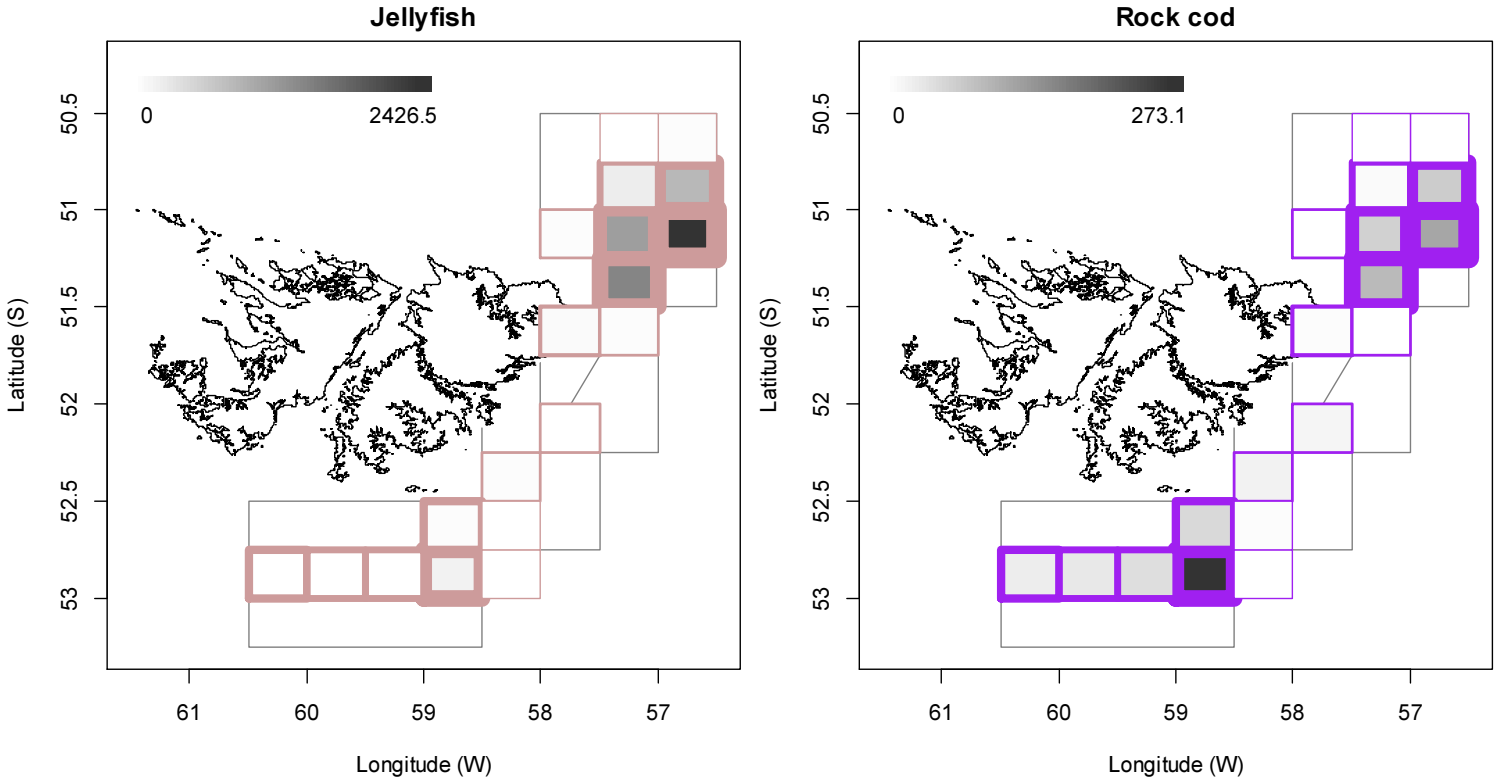

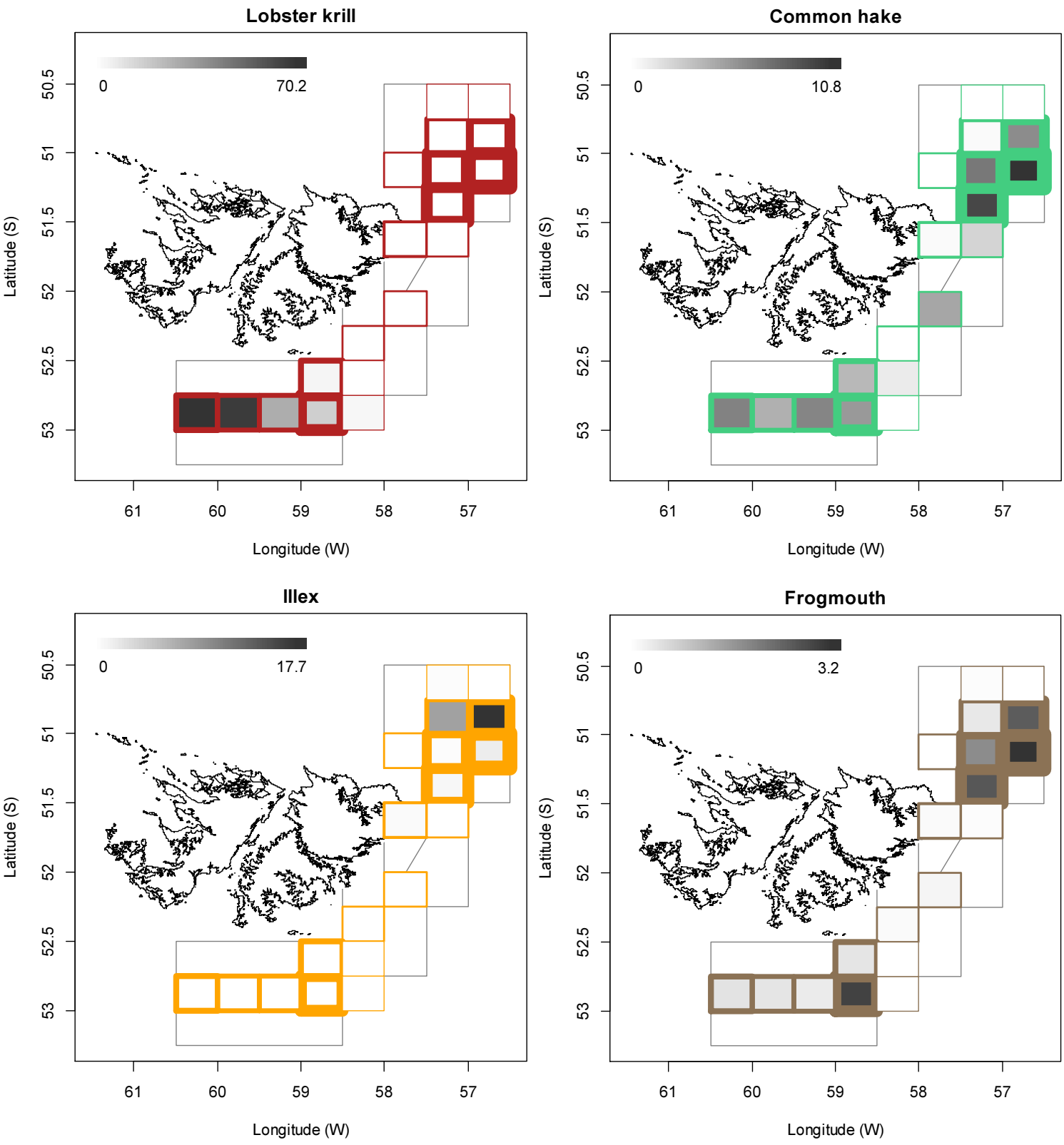
Lobster krill
0
70.2
Common hake
0
10.8
Illex
0
17.7
Frogmouth
0
3.2
Latitude (S)
50.5
51
51.5
52
52.5
53
Longitude (W)
61
60
59
58
57

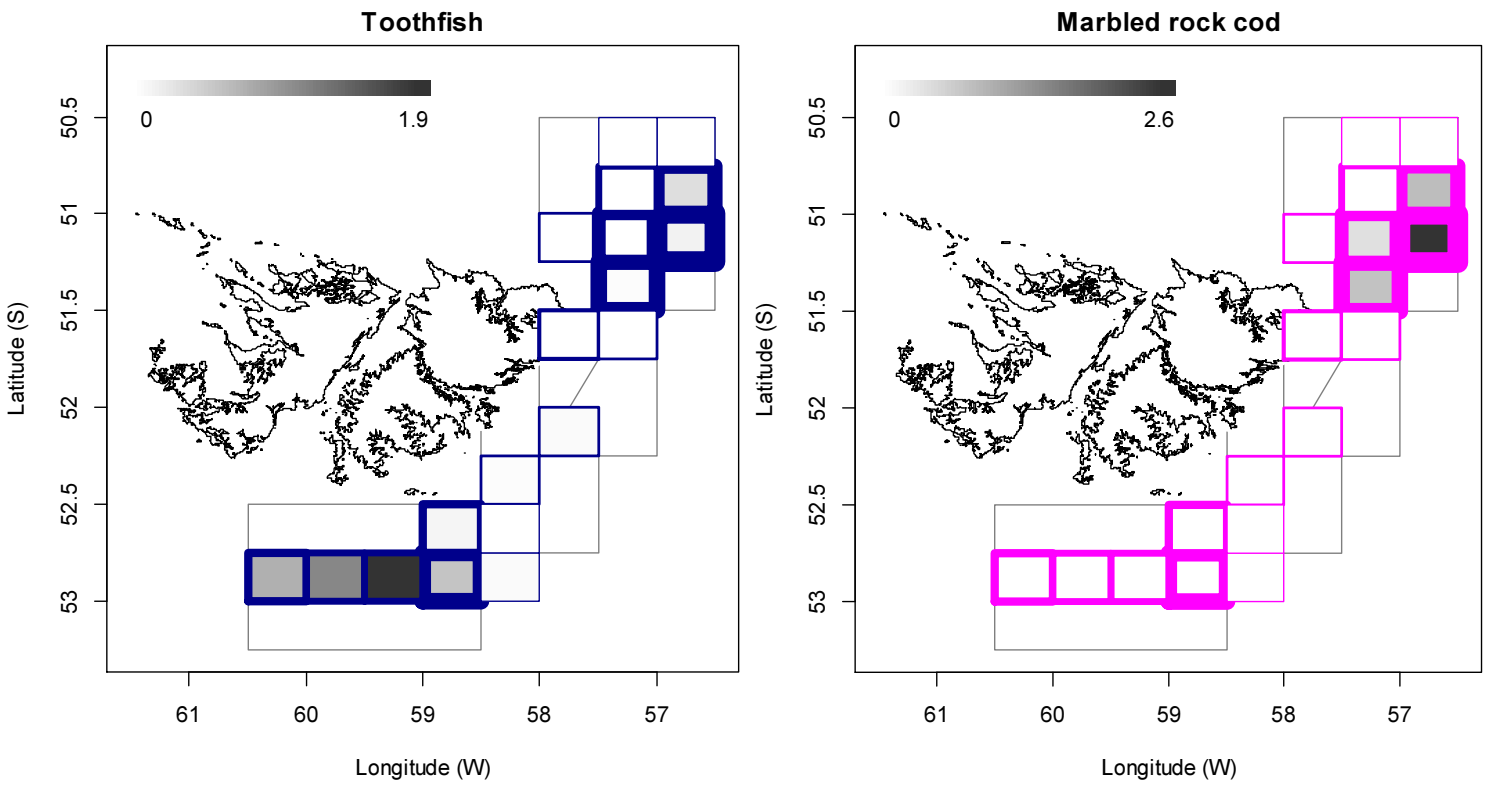

Figure 12. Distributions of the eight principal bycatches during *D. gahi* 1st season 2018, by noon position grids. Thickness of grid lines is proportional to the number of vessel-days (1 to 230 per grid; 19 different grids were occupied). Grey-scale is proportional to the bycatch biomass; maximum (tonnes) indicated on each plot.

Other high bycatches in 1st season 2018 were rock cod (*Patagonotothen ramsayi*), as usual, with 815 t from 863 vessel-days, common hake *Merluccius hubbsi* (69 t, 476 vessel-days), shortfin squid *Illex argentinus* (29 t, 128 vessel-days), frogmouth *Cottoperca gobio* (15 t, 403 vessel-days), toothfish *Dissostichus eleginoides* (5 t, 166 vessel-days), and marbled rock cod *Patagonotothen tessellata* (4.5 t, 56 vessel-days). Relative distributions by grid of these bycatches are shown in Figure 12, and the complete list of all catches by species is given in Table A1. Other than jellyfish, the only change from last 1st season's list of high bycatches (Winter 2017a) was red cod *Salilota australis*, dropping from fourth to tenth place (Table A1).

Trawl area coverage

Falkland Islands trawl fisheries, including the *D. gahi* fishery, have come under increased scrutiny for their potentially harmful effects on seafloor benthos (RSPB 2017). While a benthic impact evaluation is not within the scope of this stock assessment, the available catch, effort, and positional data can be used to summarize the estimated 'ground' area coverage occupied by a season of trawling.

The procedure for summarizing trawl area coverage is described in the Appendix. 50% of total *D. gahi* catch was taken from 0.6% of the total area of the Loligo Box,

corresponding approximately[b] to the aggregate of grounds trawled ≥17.3 times. 90% of total *D. gahi* catch was taken from 3.1% of the total area of the Loligo Box, corresponding approximately to the aggregate of grounds trawled ≥2.7 times. 100% of total *D. gahi* catch over the season was taken from 7.1% of the total area of the Loligo Box, obviously corresponding to the aggregate of all grounds trawled at least once (Figure 13 - left). Conversely, this means that 92.9% of the area of the Loligo Box was never trawled during the season. The 92.9% estimate should be seen with the caveat that it includes the sum of all patches of terrain, no matter how small, that escaped the criss-cross of trawl tracks, and not every patch of terrain is a valuable marine habitat reserve. Notwithstanding, the analysis presents an overview of how concentrated fishing may be in a season of high catches. Averaged by 5 × 5 km grid (Figure 13 - right), 8 grids (out of 1421) had coverage of 15 or more (that is to say, every patch of ground within that 5 × 5 km was on average trawled over 15 times or more). Twenty-six grids had coverage of 5 or more, and 51 grids had coverage of 2 or more.

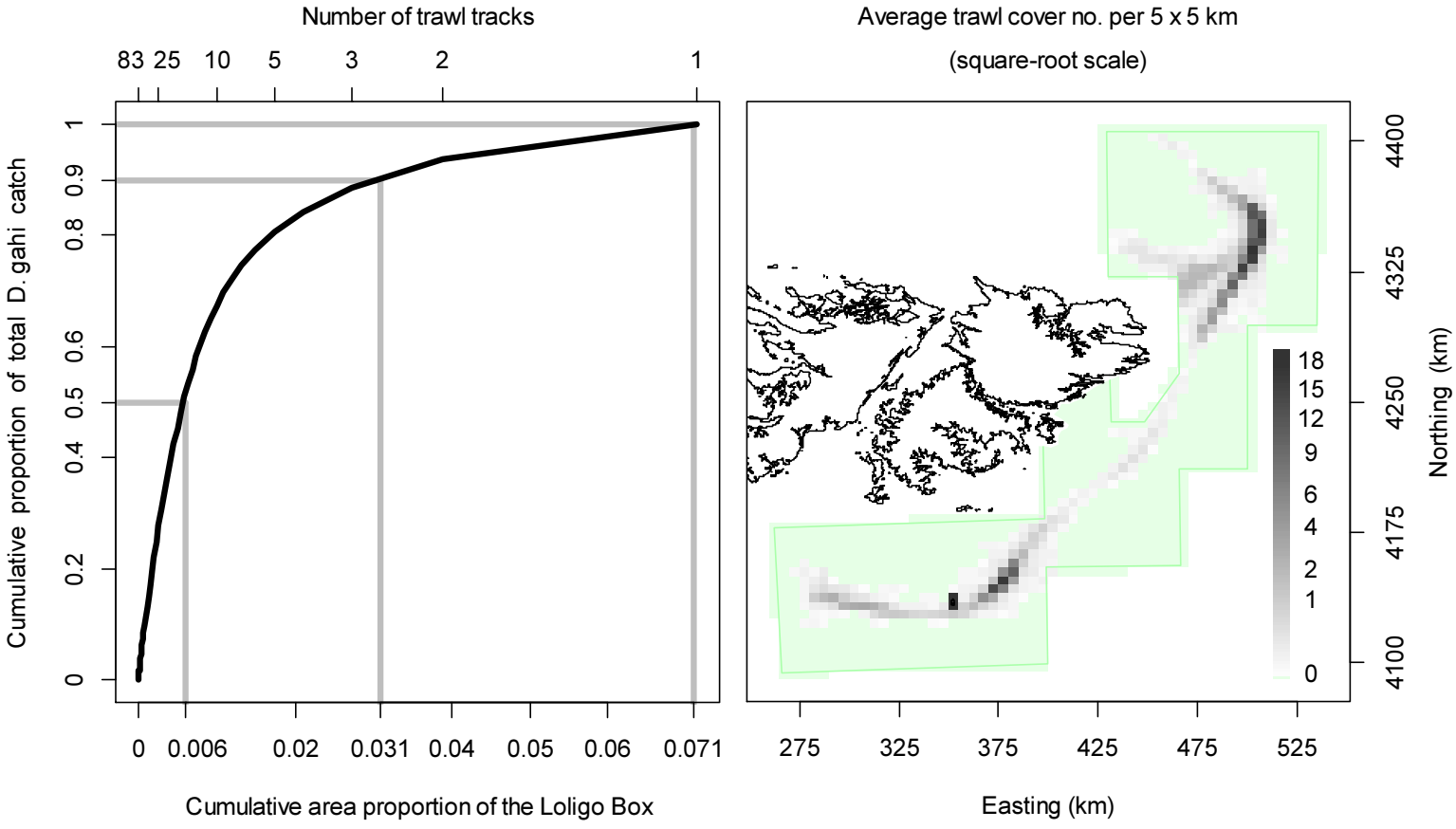

Figure 13. Left: cumulative *D. gahi* catch of 1st season 2018, vs. cumulative area proportion of the Loligo Box the catch was taken from. The maximum number of times that any single area unit was trawled was 83, and catch cumulation by reverse density corresponded approximately to the trawl multiples shown on the top x-axis. Right: trawl cover averaged by 5 × 5 km grid; green area represents zero trawling.

[b] However, not exactly. There is an expected strong correlation between the density of *D. gahi* catch taken from area units and how often these area units were trawled, but the correlation is not perfectly monotonic.

References

Agnew, D.J., Baranowski, R., Beddington, J.R., des Clers, S., Nolan, C.P. 1998. Approaches to assessing stocks of *Loligo gahi* around the Falkland Islands. Fisheries Research 35: 155-169.

Agnew, D. J., Beddington, J. R., and Hill, S. 2002. The potential use of environmental information to manage squid stocks. Canadian Journal of Fisheries and Aquatic Sciences, 59: 1851–1857.

Arkhipkin, A. 1993. Statolith microstructure and maximum age of *Loligo gahi* (Myopsida: Loliginidae) on the Patagonian Shelf. Journal of the Marine Biological Association of the UK 73: 979-982.

Arkhipkin, A.I., Middleton, D.A.J. 2002. Sexual segregation in ontogenetic migrations by the squid *Loligo gahi* around the Falkland Islands. Bulletin of Marine Science 71: 109-127.

Arkhipkin, A.I., Middleton, D.A.J., Barton, J. 2008. Management and conservation of a short-lived fishery resource: *Loligo gahi* around the Falkland Islands. American Fisheries Society Symposium 49: 1243-1252.

Arreguín-Sánchez, F. 1996. Catchability: a key parameter for fish stock assessment. Reviews in Fish Biology and Fisheries 6: 221-242.

Barton, J. 2002. Fisheries and fisheries management in Falkland Islands Conservation Zones. Aquatic Conservation: Marine and Freshwater Ecosystems 12: 127–135.

Brooks, S.P., Gelman, A. 1998. General methods for monitoring convergence of iterative simulations. Journal of computational and graphical statistics 7:434-455.

Chemshirova, I. 2018. Observer Report 1179. Technical Document, FIG Fisheries Department. 23 p.

Chen, X., Chen, Y., Tian, S., Liu, B., Qian, W. 2008. An assessment of the west winter-spring cohort of neon flying squid (*Ommastrephes bartramii*) in the Northwest Pacific Ocean. Fisheries Research 92: 221-230.

DeLury, D.B. 1947. On the estimation of biological populations. Biometrics 3: 145-167.

Gamerman, D., Lopes, H.F. 2006. Markov Chain Monte Carlo. Stochastic simulation for Bayesian inference. 2nd edition. Chapman & Hall/CRC.

Hoenig, J.M. 1983. Empirical use of longevity data to estimate mortality rates. Fishery Bulletin 82: 898-903.

Iriarte, V. 2018a. Observer Report 1185. Technical Document, FIG Fisheries Department. 23 p.

Iriarte, V. 2018b. Observer Report 1186. Technical Document, FIG Fisheries Department. 22 p.

Jiao, Y., Cortés, E., Andrews, K., Guo, F. 2011. Poor-data and data-poor species stock assessment using a Bayesian hierarchical approach. Ecological Applications 21: 2691-2708.

Keller, S., Robin, J.P., Valls, M., Gras, M., Cabanellas-Reboredo, M., Quetglas, A. 2015. The use of depletion models to assess Mediterranean cephalopod stocks under the current EU data collection framework. Mediterranean Marine Science 16: 513-523.

Kuepfer, A. 2018a. Observer Report 1181. Technical Document, FIG Fisheries Department. 32 p.

Kuepfer, A. 2018b. Observer Report 1187. Technical Document, FIG Fisheries Department. 28 p.

Magnusson, A., Punt, A., Hilborn, R. 2013. Measuring uncertainty in fisheries stock assessment: the delta method, bootstrap, and MCMC. Fish and Fisheries 14: 325-342.

Medellín-Ortiz, A., Cadena-Cárdenas, L., Santana-Morales, O. 2016. Environmental effects on the jumbo squid fishery along Baja California's west coast. Fisheries Science 82: 851-861.

Morales-Bojórquez, E., Hernández-Herrera, A., Cisneros-Mata, M.A., Nevárez-Martínez, M.O. 2008. Improving estimates of recruitment and catchability of jumbo squid *Dosidicus gigas* in the Gulf of California, Mexico. Journal of Shellfish Research 27: 1233-1237.

Nash, J.C., Varadhan, R. 2011. optimx: A replacement and extension of the optim() function. R package version 2011-2.27. http://CRAN.R-project.org/package=optimx

Patterson, K.R. 1988. Life history of Patagonian squid *Loligo gahi* and growth parameter estimates using least-squares fits to linear and von Bertalanffy models. Marine Ecology Progress Series 47: 65-74.

Payá, I. 2010. Fishery Report. *Loligo gahi*, Second Season 2009. Fishery statistics, biological trends, stock assessment and risk analysis. Technical Document, Falkland Islands Fisheries Dept. 54 p.

Pierce, G.J., Guerra, A. 1994. Stock assessment methods used for cephalopod fisheries. Fisheries Research 21: 255 – 285.

Punt, A.E., Hilborn, R. 1997. Fisheries stock assessment and decision analysis: the Bayesian approach. Reviews in Fish Biology and Fisheries 7:35-63.

Roa-Ureta, R. 2012. Modelling in-season pulses of recruitment and hyperstability-hyperdepletion in the *Loligo gahi* fishery around the Falkland Islands with generalized depletion models. ICES Journal of Marine Science 69: 1403–1415.

Roa-Ureta, R., Arkhipkin, A.I. 2007. Short-term stock assessment of *Loligo gahi* at the Falkland Islands: sequential use of stochastic biomass projection and stock depletion models. ICES Journal of Marine Science 64: 3-17.

Rosenberg, A.A., Kirkwood, G.P., Crombie, J.A., Beddington, J.R. 1990. The assessment of stocks of annual squid species. Fisheries Research 8: 335-350.

RSPB (Royal Society for the Protection of Birds). 2017. Falkland Islands fisheries detailed report 2017. ww2.rspb.org.uk/ourwork/library/reports.aspx, 54 p.

Royer, J., Périès, P., Robin, J.P. 2002. Stock assessments of English Channel loliginid squids: updated depletion methods and new analytical methods. ICES Journal of Marine Science 59: 445-457.

Shaw, P.W., Arkhipkin, A.I., Adcock, G.J., Burnett, W.J., Carvalho, G.R., Scherbich, J.N., Villegas, P.A. 2004. DNA markers indicate that distinct spawning cohorts and aggregations of Patagonian squid, *Loligo gahi*, do not represent genetically discrete subpopulations. Marine Biology, 144: 961-970.

Su, Z., Adkison, M.D., Van Alen, B.W. 2001. A hierarchical Bayesian model for estimating historical salmon escapement and escapement timing. Canadian Journal of Fisheries and Aquatic Sciences 58: 1648-1662.

Trevizan, T. 2018a. Observer Report 1193. Technical Document, FIG Fisheries Department. 25 p.

Trevizan, T. 2018b. Observer Report 1196. Technical Document, FIG Fisheries Department. 24 p.

Winter, A. 2014. *Loligo* stock assessment, second season 2014. Technical Document, Falkland Islands Fisheries Department. 30 p.

Winter, A. 2016. Falkland calamari stock assessment, first season 2016. Technical Document, Falkland Islands Fisheries Department. 27 p.

Winter, A. 2017a. Stock assessment – Falkland calamari (*Doryteuthis gahi*). Technical Document, Falkland Islands Fisheries Department. 30 p.

Winter, A. 2017b. Stock assessment – *Doryteuthis gahi* 2nd season 2017. Technical Document, Falkland Islands Fisheries Department. 37 p.

Winter, A., Arkhipkin, A. 2015. Environmental impacts on recruitment migrations of Patagonian longfin squid (*Doryteuthis gahi*) in the Falkland Islands with reference to stock assessment. Fisheries Research 172: 85-95.

Winter, A., Shcherbich, Z., Iriarte, V., Zawadowski, T. 2018. *Doryteuthis gahi* stock assessment survey, 1st season 2018. Technical Document, Falkland Islands Fisheries Department. 20 p.

Young, I.A.G., Pierce, G.J., Daly, H.I., Santos, M.B., Key, L.N., Bailey, N., Robin, J.-P., Bishop, A.J., Stowasser, G., Nyegaard, M., Cho, S.K., Rasero, M., Pereira, J.M.F. 2004. Application of depletion methods to estimate stock size in the squid *Loligo forbesi* in Scottish waters (UK). Fisheries Research 69: 211-227.

Zhang, H.-M., Bates, J.J., Reynolds, R.W. 2006. Assessment of composite global sampling: Sea surface wind speed. Geophysical Research Letters 33: L17714.

Appendix
***Doryteuthis gahi* individual weights**

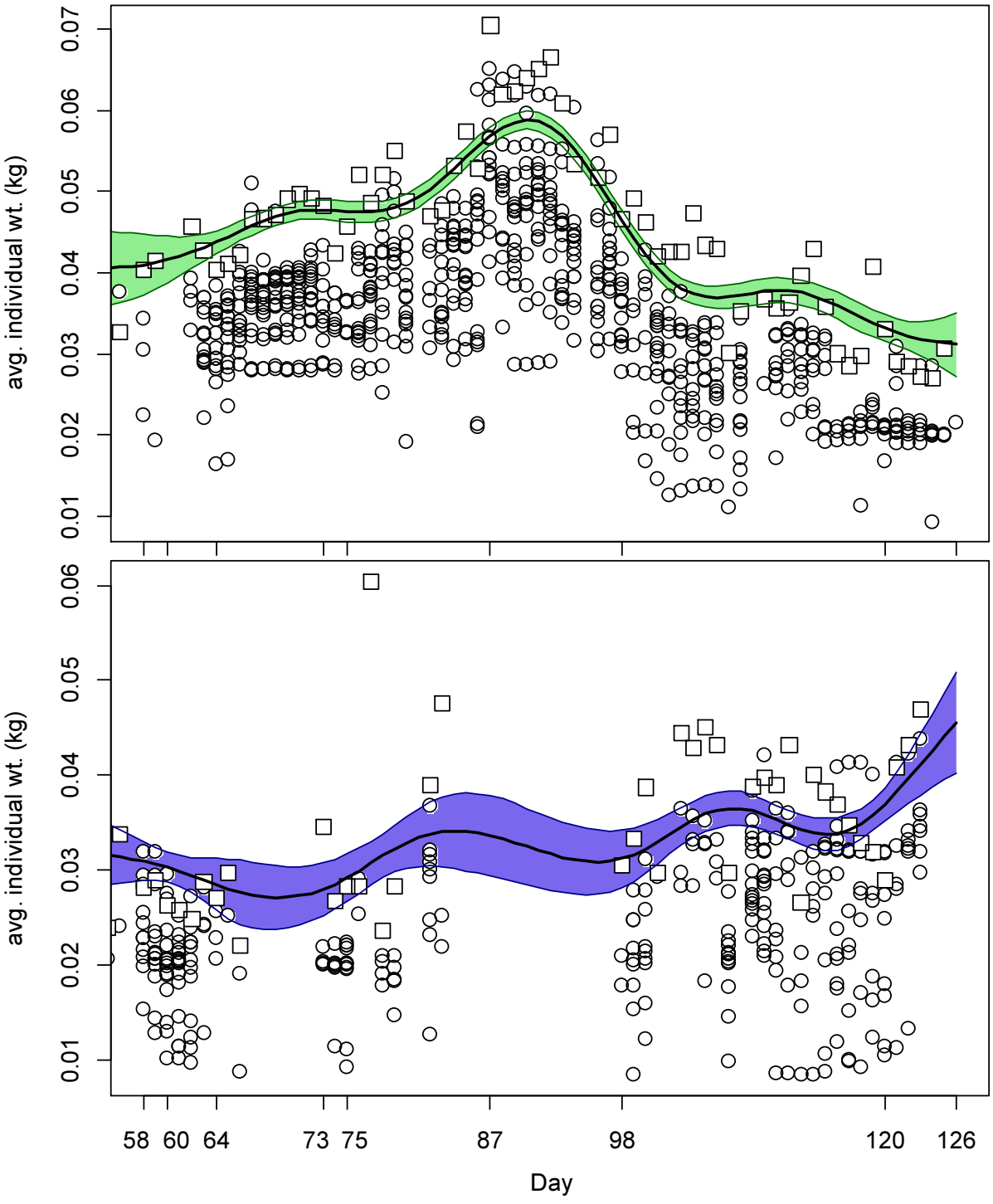

Figure A1. North (top) and south (bottom) sub-area daily average individual *D. gahi* weights from commercial size categories per vessel (circles) and observer measurements (squares). GAMs of the daily trends ± 95% confidence intervals (centre lines and colour under-shading).

To smooth fluctuations, generalized additive model (GAM) trends were calculated of daily average individual weights. North and south sub-areas were calculated separately. For

continuity, the GAMs were calculated using all pre-season survey and in-season data contiguously. North and south GAMs were first calculated separately on the commercial and observer data. The commercial data GAMs were taken as the baseline trends, and calibrated to the observer data GAMs in proportion to the correlation between the commercial data and observer data GAMs. For example, if the season average individual weight estimate from commercial data was 0.052 kg, the season average individual weight estimate from observer data was 0.060 kg, and the coefficient of determination (R^2) between commercial and observer GAM trends was 86%, then the resulting trend of daily average individual weights was calculated as the commercial data GAM values + (0.060 – 0.052) × 0.86. This way, both the greater day-to-day consistency of the commercial data trends, and the greater point value accuracy of the observer data are represented in the calculations. GAM plots of the north and south sub-areas are shown in Figure A1.

Prior estimates and CV

The pre-season survey (Winter et al. 2018) had estimated *D. gahi* biomasses of 569 t (standard deviation: ± 1,263 t) north of 52º S and 31,625 t (standard deviation: 18,866 t) south of 52º S. From modelled survey catchability, Payá (2010) had estimated average net escapement of up to 22%, which was added to the standard deviation:

$$569 \pm \left(\frac{1263}{569} + .22\right) = 569 \pm 244.0\% \quad = 569 \pm 1{,}388 \text{ t} \qquad \textbf{(A1-N)}$$

$$31{,}625 \pm \left(\frac{18{,}866}{31{,}625} + .22\right) = 31{,}625 \pm 81.7\% \quad = 31{,}625 \pm 25{,}824 \text{ t} \qquad \textbf{(A1-S)}$$

$$32{,}194 \pm \left(\frac{18{,}472}{32{,}194} + .22\right) = 32{,}194 \pm 79.4\% \quad = 32{,}194 \pm 25{,}555 \text{ t} \qquad \textbf{(A1-C)}$$

The 22% was added as a linear increase in the variability, but was not used to reduce the total estimate, because squid that escape one trawl are likely to be part of the biomass concentration that is available to the next trawl.

D. gahi numbers at the end of the survey were estimated as the survey biomasses divided by the GAM-predicted individual weight averages for the survey: 0.0407 kg north, 0.0341 kg south (Figure A1), and 0.0350 kg combined. Average coefficients of variation (CV) of the GAM over the duration of the pre-season survey were 5.7% north, 7.0% south and 5.4% combined. CV of the length-weight conversion relationship (Equation **8**) were 6.1% north, 6.1% south, and 6.1% combined. Joining these sources of variation with the pre-season survey biomass estimates and individual weight averages (above) gave estimated *D. gahi* numbers at survey end (day 56) of:

$$_{\text{prior}}N_{\text{N day 56}} = \frac{569 \times 1000}{0.0407} \pm \sqrt{244.0\%^2 + 5.7\%^2 + 6.1\%^2}$$

$$= 0.014 \times 10^9 \pm 244.2\%$$

$$_{\text{prior}}N_{\text{S day 56}} = \frac{31{,}625 \times 1000}{0.0341} \pm \sqrt{81.7\%^2 + 7.0\%^2 + 6.1\%^2}$$

$$= 0.926 \times 10^9 \pm 82.2\%$$

$$_{\text{prior}}N_{\text{C day 56}} = \frac{32{,}194 \times 1000}{0.0350} \pm \sqrt{79.4\%^2 + 5.4\%^2 + 6.1\%^2}$$

$$= 0.921 \times 10^9 \pm 79.8\%$$

North and south priors were normalized for the combined fishing zone average, to produce better continuity as vessels cross back and forth between north and south:

$$_{\text{nprior}}N_{\text{N day 56}} = \left(\frac{(569 + 31{,}625) \times 1000}{0.0350}\right) \times \left(\frac{_{\text{prior}}N_{\text{N day 56}}}{_{\text{prior}}N_{\text{N day 56}} + _{\text{prior}}N_{\text{S day 56}}}\right)$$

$$= 0.014 \times 10^9 \pm 244.2\% \quad \textbf{(A2-N)}$$

$$_{\text{nprior}}N_{\text{S day 56}} = \left(\frac{(31{,}625 + 569) \times 1000}{0.0350}\right) \times \left(\frac{_{\text{prior}}N_{\text{S day 56}}}{_{\text{prior}}N_{\text{N day 56}} + _{\text{prior}}N_{\text{S day 56}}}\right)$$

$$= 0.907 \times 10^9 \pm 82.2\% \quad \textbf{(A2-S)}$$

The catchability coefficient (q) prior for the north sub-area was calculated on day 58, when three vessels first fished north and the initial depletion period north started. Abundance on day 58 was discounted for natural mortality over the 2 days since the end of the survey:

$$_{\text{nprior}}N_{\text{N day 58}} = {}_{\text{nprior}}N_{\text{N day 56}} \times e^{-M \cdot (58-56)} - \text{CNMD}_{\text{N day 58}} = 0.013 \times 10^9 \quad \textbf{(A3-N)}$$

where $\text{CNMD}_{\text{N day 58}} = 0$ as no catches had been taken between day 56 and day 58. Thus:

$$_{\text{prior}}q_{\text{N}} = C(N)_{\text{N day 58}} / ({}_{\text{nprior}}N_{\text{N day 58}} \times E_{\text{N day 58}})$$

$$= (C(B)_{\text{N day 58}} / \text{Wt}_{\text{N day 58}}) / ({}_{\text{nprior}}N_{\text{N day 58}} \times E_{\text{N day 58}})$$

$$= (65.0 \text{ t} / 0.0410 \text{ kg}) / (0.013 \times 10^9 \times 3 \text{ vessel-days})$$

$$= 3.968 \times 10^{-2} \text{ vessels}^{-1} \quad \textbf{(A4-N)}$$

The value of $_{\text{prior}}q_{\text{N}}$ (**A4-N**) was exceptionally high by an order of magnitude (e.g., Winter 2016, Winter 2017a). It was judged to be an inapplicable value as the progressing season showed that catches in the north sub-area had little relationship to the pre-season biomass estimate. Therefore a weighted average catchability of north + south on day 58 was substituted as the prior for the north:

$$_{\text{prior}}q_{\text{C}} = \frac{\left(C(N)_{\text{N day 58}} + C(N)_{\text{S day 58}}\right)}{\left(\left({}_{\text{nprior}}N_{\text{N day 58}} \times E_{\text{N day 58}}\right) + \left({}_{\text{nprior}}N_{\text{S day 58}} \times E_{\text{S day 58}}\right)\right)}$$

$$= 1.514 \times 10^{-3} \text{ vessels}^{-1} \text{ [c]} \quad \textbf{(A4-C)}$$

The corresponding CV of the north + south prior was calculated as:

[c] On Figure 7-left.

$CV_{prior\ C}$ =

$$\sqrt{79.8\%^2 + \left(\frac{SD\left(C(B)_{C\ vessels\ day\ 58}\right)}{mean\left(C(B)_{C\ vessels\ day\ 58}\right)}\right)^2 + (1 - sign(1 - CV_M) \times abs(1 - CV_M)^{(58-56)})^2}$$

$$= \sqrt{79.8\%^2 + 39.4\%^2 + 28.5\%^2} \quad = 93.5\% \qquad \textbf{(A5-C)}$$

The catchability coefficient (q) prior for the south sub-area was taken on day 58, the first day of the season, when 12 vessels fished in the south and the initial depletion period south started. Abundance on day 58 was discounted for natural mortality over the 2 days since the end of the survey:

$$_{nprior}N_{S\ day\ 58} = {}_{nprior}N_{S\ day\ 58} \times e^{-M\cdot(58-56)} - CNMD_{S\ day\ 58} = 0.884 \times 10^9 \qquad \textbf{(A3-S)}$$

where $CNMD_{S\ day\ 58}$ = 0 as no catches intervened between the end of the survey and the start of commercial season. Thus:

$$_{prior}q_S = C(N)_{S\ day\ 58} / ({}_{nprior}N_{S\ day\ 58} \times E_{S\ day\ 58})$$

$$= (C(B)_{S\ day\ 58} / Wt_{S\ day\ 58}) / ({}_{nprior}N_{S\ day\ 58} \times E_{S\ day\ 58})$$

$$= (449.4\ t / 0.0309\ kg) / (0.884 \times 10^9 \times 12\ vessel\text{-}days)$$

$$= 1.370 \times 10^{-3}\ vessels^{-1}\ d \qquad \textbf{(A4-S)}$$

CV of the prior was calculated as the sum of variability in $_{nprior}N_{S\ day\ 56}$ (Equations **A2-S**) plus variability in the catches of vessels on start day 58, plus variability of the natural mortality (see Appendix section Natural mortality, below):

$CV_{prior\ S}$ =

$$\sqrt{82.2\%^2 + \left(\frac{SD\left(C(B)_{S\ vessels\ day\ 58}\right)}{mean\left(C(B)_{S\ vessels\ day\ 58}\right)}\right)^2 + (1 - sign(1 - CV_M) \times abs(1 - CV_M)^{(58-56)})^2}$$

$$= \sqrt{82.2\%^2 + 33.4\%^2 + 28.5\%^2} \quad = 93.2\% \qquad \textbf{(A5-S)}$$

Depletion model estimates and CV

For the north sub-area, the equivalent of Equation **3** with four N_{day} was optimized on the difference between predicted catches and actual catches (Equation **4**), resulting in parameter values:

$_{depletion}N1_{N\ day\ 58}$ = 2.948×10^9; $_{depletion}N2_{N\ day\ 64}$ = 1.570×10^9
$_{depletion}N3_{N\ day\ 75}$ = 0.039×10^9; $_{depletion}N4_{N\ day\ 87}$ = 1.477×10^9

[d] On Figure 9-left.

$$\text{depletion } q_{\text{N NSED}} = 0.277 \times 10^{-3}\ ^{e}$$
$$\text{depletion } q_{\text{N SED}} = 0.416 \times 10^{-3} \quad \textbf{(A6-N)}$$

The root-mean-square deviation of predicted vs. actual catches was calculated as the CV of the model:

$$CV_{\text{rmsd N}} = \frac{\sqrt{\sum_{i=1}^{n}\left({}_{\text{predicted}}C(N)_{\text{N day i}} - {}_{\text{actual}}C(N)_{\text{N day i}}\right)^2 / n}}{\text{mean}\left({}_{\text{actual}}C(N)_{\text{N day i}}\right)}$$

$$= 3.412 \times 10^{6} / 9.332 \times 10^{6} = 36.6\% \quad \textbf{(A7-N)}$$

$CV_{\text{rmsd N}}$ was added to the variability of the GAM-predicted individual weight averages for the season (Figure A1-N); equal to a CV of 1.7% north. CVs of the depletion were then calculated as the sum:

$$CV_{\text{depletion N}} = \sqrt{CV_{\text{rmsd N}}^{\ 2} + CV_{\text{GAM Wt N}}^{\ 2}} = \sqrt{36.6\%^2 + 1.7\%^2}$$
$$= 36.6\% \quad \textbf{(A8-N)}$$

For the south sub-area, the equivalent of Equation **3** with five N_{day} was optimized on the difference between predicted catches and actual catches (Equation **4**), resulting in parameters values:

$$\text{depletion } N1_{\text{S day 58}} = 0.348 \times 10^{9}; \quad \text{depletion } N2_{\text{S day 60}} = 1.052 \times 10^{1}$$
$$\text{depletion } N3_{\text{S day 73}} = 0.338 \times 10^{9}; \quad \text{depletion } N4_{\text{S day 98}} = 7.658 \times 10^{1}$$
$$\text{depletion } N5_{\text{S day 120}} = 0.057 \times 10^{9}$$
$$\text{depletion } q_{\text{S NSED}} = 3.844 \times 10^{-3}\ ^{f}$$
$$\text{depletion } q_{\text{S SED}} = 5.361 \times 10^{-3} \quad \textbf{(A6-S)}$$

The normalized root-mean-square deviation of predicted vs. actual catches was calculated as the CV of the model:

$$CV_{\text{rmsd S}} = \frac{\sqrt{\sum_{i=1}^{n}\left({}_{\text{predicted}}C(N)_{\text{S day i}} - {}_{\text{actual}}C(N)_{\text{S day i}}\right)^2 / n}}{\text{mean}\left({}_{\text{actual}}C(N)_{\text{S day i}}\right)}$$

$$= 2.282 \times 10^{6} / 4.795 \times 10^{6} = 47.6\% \quad \textbf{(A7-S)}$$

$CV_{\text{rmsd S}}$ was added to the variability of the GAM-predicted individual weight averages for the season (Figure A1-S); equal to a CV of 3.7% south. CVs of the depletion were then calculated as the sum:

$$CV_{\text{depletion S}} = \sqrt{CV_{\text{rmsd S}}^{\ 2} + CV_{\text{GAM Wt S}}^{\ 2}} = \sqrt{47.6\%^2 + 3.7\%^2}$$

[e] On Figure 7-left.
[f] On Figure 9-left.

$$= \quad 47.7\% \qquad \textbf{(A8-S)}$$

Combined Bayesian models

For the north sub-area, joint optimization of Equations **4** and **5** resulted in parameters values:

$$\begin{aligned} {}_{\text{Bayesian}}N1_{\text{N day 58}} &= 0.752 \times 10^{9}; & {}_{\text{Bayesian}}N2_{\text{N day 64}} &= 0.475 \times 10^{9} \\ {}_{\text{Bayesian}}N3_{\text{N day 75}} &= 0.117 \times 10^{9}; & {}_{\text{Bayesian}}N4_{\text{N day 87}} &= 0.592 \times 10^{9} \\ {}_{\text{Bayesian}}q_{\text{N NSED}} &= 1.086 \times 10^{-3}\,{}^{g} \\ {}_{\text{Bayesian}}q_{\text{N SED}} &= 1.902 \times 10^{-3} \end{aligned} \qquad \textbf{(A9-N)}$$

These parameters produced the fit between predicted catches and actual catches shown in Figure A2-N.

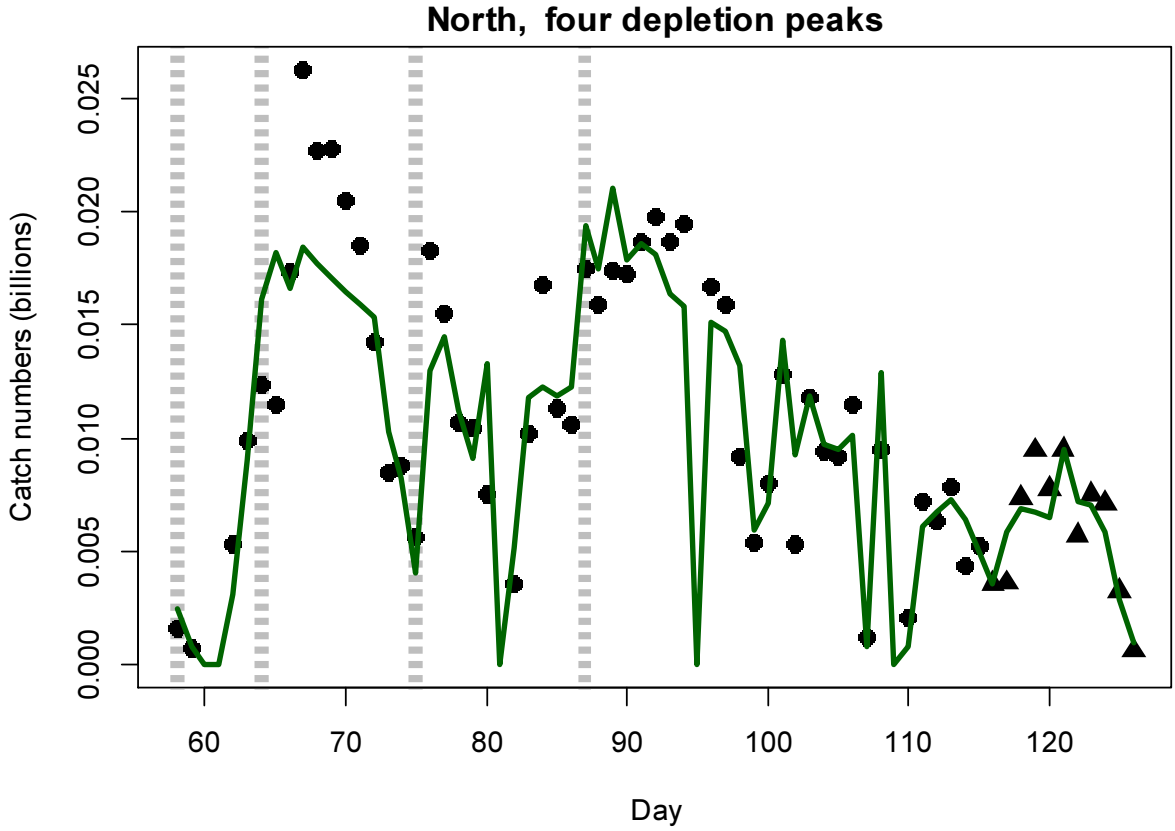

Figure A2-N. Daily catch numbers estimated from actual catch (black points: without SEDs, black triangles: with SEDs) and predicted from the depletion model (green line) in the north sub-area.

For the south sub-area, the joint optimization of Equations **4** and **5** resulted in parameters values:

$$\begin{aligned} {}_{\text{Bayesian}}N1_{\text{S day 58}} &= 0.684 \times 10^{9}; & {}_{\text{Bayesian}}N2_{\text{S day 60}} &= 1.892 \times 10^{2} \\ {}_{\text{Bayesian}}N3_{\text{S day 73}} &= 0.518 \times 10^{9}; & {}_{\text{Bayesian}}N4_{\text{S day 98}} &= 1.998 \times 10^{1} \\ {}_{\text{Bayesian}}N5_{\text{S day 120}} &= 0.034 \times 10^{9} \end{aligned}$$

[g] On Figure 7-left.

$$\text{Bayesian } q_{\text{S NSED}} = 1.737 \times 10^{-3} \text{ [h]}$$
$$\text{Bayesian } q_{\text{S SED}} = 2.335 \times 10^{-3} \quad \textbf{(A9-S)}$$

These parameters produced the fit between predicted catches and actual catches shown in Figure A2-S.

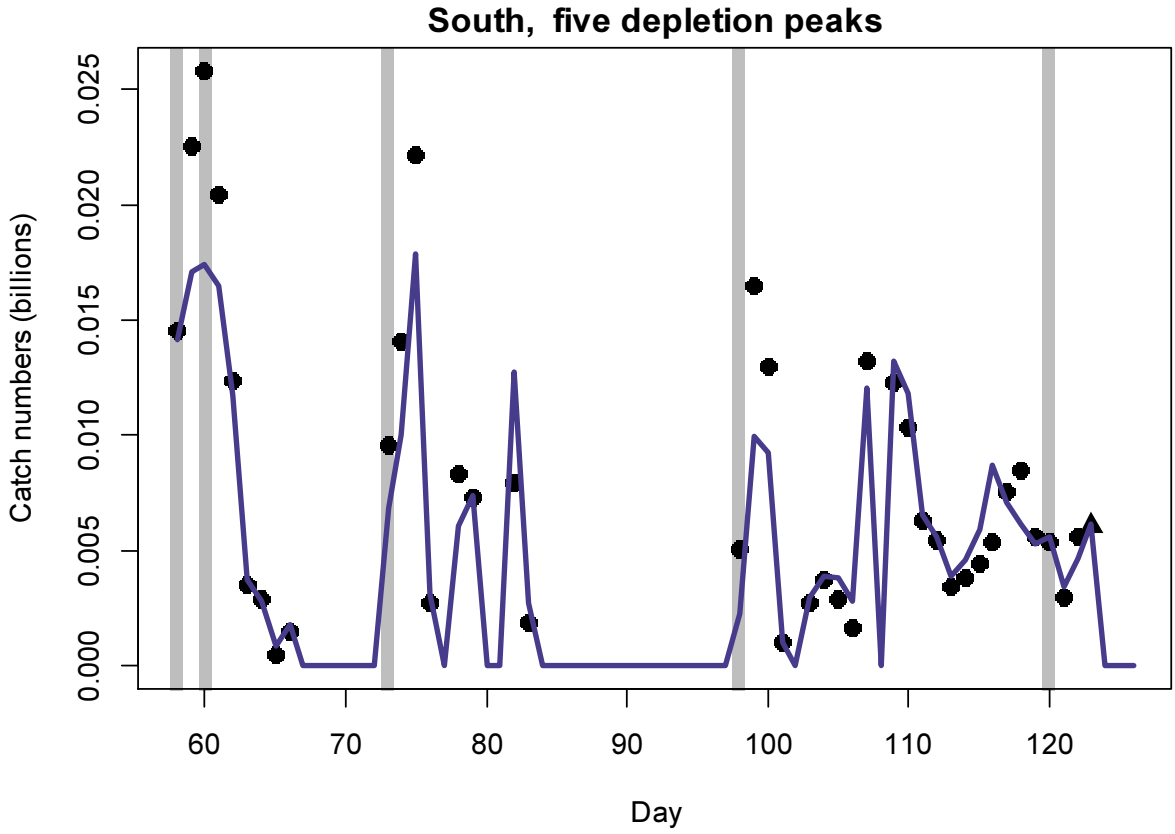

Figure A2-S. Daily catch numbers estimated from actual catch (black points: without SEDs, black triangles: with SEDs) and predicted from the depletion model (purple line) in the south sub-area.

Natural mortality

Natural mortality is parameterized as a constant instantaneous rate M = 0.0133 day^{-1} (Roa-Ureta and Arkhipkin 2007), based on Hoenig's (1983) log mortality vs. log maximum age regression applied to an estimated maximum age of 352 days for *Doryteuthis gahi*:

$$\log(M) = 1.44 - 0.982 \times \log(\text{age}_{\max})$$
$$M = \exp(1.44 - 0.982 \times \log(352))$$
$$= 0.0133 \quad \textbf{(A10)}$$

Hoenig (1983) derived Equation **A10** from the regression of 134 stocks among 79 species of fish, molluscs, and cetaceans. Hoenig's regression obtained $R^2 = 0.82$, but a corresponding

[h] On Figure 9-left.

coefficient of variation (CV) was not published. A CV of M was estimated by measuring the coordinates off a print of Figure 1 in Hoenig (1983) and repeating the regression. Variability of M was calculated by randomly re-sampling, with replacement, the regression coordinates 10000× and re-computing Equation **A10** for each iteration of the resample (Winter 2017a). The CV of M from the 10000 random resamples was:

$$CV_M = SD_M / Mean_M$$

$$CV_M = 0.0021 / 0.0134 = 15.46\% \quad \textbf{(A11)}$$

CV_M over the aggregate number of unassessed days between survey end and commercial season start was then added to the CV of the biomass prior estimate and the CV of variability in vessel catches on start day (**A5-S** and **A5-N**). CV_M was further expressed as an absolute value and indexed by sign(1 - CV_M) to ensure that the value could not decrease if CV_M was hypothetically > 100% (**A5-S**).

Trawl area coverage

Area coverage was defined as the length of trawls × their trawl door width. For each of the 3078 trawls taken during the season (Figure 3), trawl door widths were obtained from the vessels' fishing reports. Missing trawl door widths were assigned as the average for that vessel for the season. The area cover of each trawl was then calculated as the rectangle of half the trawl width on either side of the start to end positions recorded for the trawl. This calculation implies the trawl to have been linear. However, if the Euclidean (straight-line) distance between start and end position was less than 80% of the trawl's timed distance (duration × average speed), the trawl was assumed to have turned, and for calculation was split on a pivot point. As turns are not reported, there is no direct way to infer the pivot point. Instead, the pivot point was optimized as the coordinate that produced an aggregate distance to the trawl start position + to the trawl end position most closely matching the timed distance of the trawl, with the constraint that this coordinate could not lie outside the 'box' of where the vessel had been over the period from the day before to the day after.

The rectangular areas of all trawls and split-trawls were then projected onto the Loligo Box. To estimate the areal proportion covered, the Loligo Box was discretized on a scale of 3 × 3 m. To make the amount of data points this produced tractable, the Loligo Box was further subdivided into grids of 5 × 5 km. As border grids intersected the Loligo Box, for each grid the actual number of points located within the Loligo Box (maximum (5000 × 5000)/(3 × 3) = 2778889 points) was first calculated by using the 'point.in.polygon' function of R package 'sp', both on the delineation of the Loligo Box (inclusively) and on the delineation of the Beauchêne Island Zone (exclusively). Then, any points were eliminated that corresponded to water depth of <10 m, interpolated from a GEBCO_08 30 arc-second bathymetry grid (British Oceanographic Data Centre). Finally, the grid was looped through the projection of each trawl and split-trawl area by turn[i], and again using 'point.in.polygon', the points covered by each trawl / split-trawl were iteratively summed. For all rectangulations and area calculations, coordinates were converted to WGS 84 projection in UTM sector 21F using R library 'rgdal' (proj.maptools.org).

Outputs derived from the calculations were the total area proportion of the Loligo Box trawled, the cumulative numbers of trawl passes over any proportion of the Loligo Box, the

[i] In practice, to reduce computer time subsets of trawls were preselected that intersected each given grid.

concentration of *D. gahi* catch by area proportion of the Loligo Box, and the concentration of effort by area proportion of the Loligo Box.

Total catch by species

Table A1: Total reported catches and discard by taxon during second season 2017 *Doryteuthis gahi* fishing, and number of catch reports in which each taxon occurred. Does not include incidental catches of pinnipeds.

Species Code	Species / Taxon	Catch Wt. (KG)	Discard Wt. (KG)	N Reports
LOL	*Doryteuthis gahi*	43085394	17847	975
MED	Medusae spp.	6462775	6462775	772
PAR	*Patagonotothen ramsayi*	814784	813662	863
MUN	*Munida* spp.	195485	195485	160
HAK	*Merluccius hubbsi*	68553	7204	476
ILL	*Illex argentinus*	29158	1642	128
CGO	*Cottoperca gobio*	15283	15163	403
TOO	*Dissostichus eleginoides*	4935	2453	166
PTE	*Patagonotothen tessellata*	4565	4565	56
BAC	*Salilota australis*	3231	385	66
ALF	*Allothunnus fallai*	3193	2995	164
SCA	scallop	1947	1947	26
RAY	Rajidae	1709	1684	250
GRV	*Macrourus* spp.	1390	1390	10
ING	*Moroteuthis ingens*	1324	1324	100
CHE	*Champsocephalus esox*	984	984	97
KIN	*Genypterus blacodes*	753	753	100
DGH	*Schroederichthys bivius*	710	710	59
SAR	*Sprattus fuegensis*	494	494	7
SPN	Porifera	213	213	8
POR	*Lamna nasus*	200	200	3
UCH	Sea urchin	128	128	5
OCT	*Octopus* spp.	47	47	13
DGS	*Squalus acanthias*	37	37	5
WHI	*Macruronus magellanicus*	26	26	9
GRC	*Macrourus carinatus*	26	26	3
OTH	–	22	22	4
MYX	*Myxine* spp.	17	17	5
BDU	*Brama dussumieri*	12	12	3
GRX	*Coelorhynchus* sp. cf. *braueri*	12	12	1
DIM	*Dissostichus mawsoni*	10	4	10
LIM	*Lithodes santolla*	10	10	2
DGX	Dogfish / catshark	8	8	1
RED	*Sebastes oculatus*	4	4	2
PAT	*Merluccius australis*	3	3	1
NEM	*Neophyrnichthys marmoratus*	1	1	1
Total		50697443	7534232	4954